IN-VIVO STUDY OF INHIBITION IN THE HUMAN HIPPOCAMPUS

KENNETH PATRICK VIVES

Yale University

1995

In-Vivo Study of Inhibition in the Human Hippocampus

A Thesis Submitted to the Yale University School of Medicine in Partial Fulfillment of the Requirements for the Degree of Doctor of Medicine

by

Kenneth Patrick Vives

1995

ABSTRACT

IN-VIVO STUDY OF INHIBITION IN THE HUMAN HIPPOCAMPUS. Kenneth P. Vives, Gregory McCarthy and Dennis D. Spencer. Section of Neurosurgery, Yale University School of Medicine, New Haven, CT.

Loss of inhibition has been shown to be associated with histological changes and epileptic activity of the hippocampus. Twenty-three patients undergoing anteromedial temporal resection for intractable epilepsy underwent an intraoperative electrophysiological study to measure inhibition. These patients were split into two groups: patients with lesions related to medial temporal lobe epilepsy (LRMTLE) and patients with mesial temporal sclerosis (MTS). Prior to hippocampal resection a stimulating electrode was placed in the perforant path and a recording electrode through the dentate gyrus. At interstimulus intervals (ISI's) of 20, 40, 60, 100, 200 msec, the amount of feedback inhibition was quantified by calculating the ratio of the size of the exictatory post synaptic potential (EPSP) and the population spike (PS) to that elicited by a single stimulus. At frequencies of 0.2, 0.5, 1, 2 and 3 Hz the amount of frequency-related inhibition was quantified by the ratio of the PS or EPSP to that elicited at 0.1 Hz. The results revealed a loss of feedback inhibition at an ISI of 20 msec for the MTS patients compared to the LRMTLE patients ($p = 0.0018$). This loss of was further shown to be directly correlated with hippocampal atrophy as measured by MRI volumetrics and the number of years of seizures ($r = 0.819$ and 0.883). A loss of feedforward inhibition at 1 Hz was found in both sets of patients. The MTS patients showed an abnormal frequency related attenuation at higher frequencies compared to the LRMTLE patients ($p = 0.0240$). These findings are consistent with an excitotoxic

loss of activity-dependent cells in a feedforward circuit in the LRMTLE patients and a loss of excitatory mossy cells in the dentate gyrus hilus of patients with MTS. This information contributes to the understanding of normal inhibition in the intact hippocampus and may possibly aid in the treatment of patients with intractable medial temporal lobe epilepsy.

ACKNOWLEDGMENTS

I would like to acknowledge the patients, who knowingly participated in this study in order to further our understanding of epilepsy in the hope that this knowledge could be used to help others. I would also like to thank: Dr. Gregory McCarthy for his limitless support, advice, thoughtful input and inherent trust in allowing me the freedom to perform this study with independence; Dr. Nihal de Lanerolle for his contribution of time in assisting in the location of lesions and his contribution of immunohistochemical data; Dr. Jung Kim for all of his teaching, support and the contribution of cell count data; Dr. Anne Williamson for the sharing of her electrophysiological expertise, insights and review of the manuscript; Marie Luby for her general help, friendship and assistance with the hippocampal volumetric data, Joseph Jasiorkowski for his assistance in the OR and all of his electronic expertise; the rest of the members of the Neuropsychology Lab, who all at one time or another gave thoughtful advice and assistance; all of the fellows and residents who patiently gave their time and expertise in length estimation; and Dr. Susan Spencer from whose ideas this study was conceived.

I would also like to acknowledge my family for their continual support and encouragement and Alison Moriarty for her careful review of the manuscript, support, tolerance and understanding.

Lastly, I would like to acknowledge Dr. Dennis Spencer, my mentor and role-model for the last two years who gave a seemingly limitless amount of time and effort in every step of this project, placed the electrodes for each experiment and provided a detailed review of the manuscript.

> "Men nearly always follow the tracks made by others and proceed in their affairs by imitation, even though they cannot entirely keep to the tracks of others or emulate the prowess of their models. So a prudent man should always follow in the footsteps of great men and imitate those who have been outstanding."
>
> - Niccolò Machiavelli (1469–1527)

TABLE OF CONTENTS

INTRODUCTION

Epilepsy as a Disease Process

Epilepsy is a disease process that affects approximately one percent of the population. Forty to fifty-five percent of these patients have seizures that are classified as complex partial (Gastaut, et al., 1975; Hauser and Kurkland, 1975). Intracranial depth electrode studies have confirmed that most complex partial seizures originate from the temporal lobe (Engel, et al., 1975; Engel, 1981; Spencer, et al., 1982; Spencer, et al., 1990). Up to 2/3 of patients with temporal lobe epilepsy eventually become refractory to medical management and are considered surgical candidates. These patients may be divided into two groups: those patients with mass lesions in the temporal lobe associated with their epilepsy and those patients without (Spencer, 1994). The vast majority of the latter group are identified as having mesial temporal sclerosis (MTS) associated with their seizures, while the former group includes patients with low grade tumors, vascular lesions and developmental lesions (Spencer, et al., 1984a).

In common, all of these patients have an underlying substrate that permits the generation of recurrent seizures (Spencer, 1994). Evidence of the manifestations of this substrate may be sought anatomically, histologically, and functionally. Tumors or atrophy of the temporal lobe or hippocampus may be observed both through imaging and at surgery. Careful volumetric measurements of the hippocampus may quantify this atrophy and allow comparisons with a control population (Lencz, et al., 1992). Pathological examination of surgical specimens may reveal a neoplastic process, a vascular malformation or neuronal loss and gliosis in a pattern typical of MTS (Spencer, 1994). Additionally, immunohistochemical study may reveal changes in the distribution of neurotransmitters and reorganization (de Lanerolle, et al., 1992).

Dysfunction may be evident in several different ways. Neuropsychological impairment may be found on cognitive testing (Sass, et al., 1990; Sass, et al., 1992).

Disturbances of glucose metabolism may be evident on 18-flurorodeoxyglucose positron emission tomography (FDG-PET) (Henry, et al., 1993). Lastly, the patient may manifest the disorder not only through seizures, which in themselves are relatively infrequent events, but through other electrophysiological abnormalities that may be more or less constant. These may include disturbances of normally evoked responses to cognitive stimuli, the presence of spontaneous interictal epileptiform discharges or through electrophysiological paradigms designed to study inhibition. Dysfunctional inhibition may contribute to the previously mentioned problems and is thought to play a role in allowing the patient to move from an inter-ictal to an ictal state. Our goal was to study the presence or absence of inhibition in the human hippocampus at the time of surgery for intractable medial temporal lobe epilepsy and compare the results between these two subsets of patients: patients with MTS and patients with lesion related medial temporal lobe epilepsy. Additionally, these findings were correlated with a number of other ancillary variables that could also possibly contribute to the findings.

In the following sections, the normal anatomy, circuitry and relevant neurotransmitters of the hippocampus will be described. This will be followed by a discussion of the relevant electrophysiological paradigms used to study inhibition in the context of the known anatomical circuits and biochemistry. Evidence will be presented for a loss of inhibition in the context of epilepsy through pathological, immunohistochemical and electrophysiological changes in animal models of epilepsy and in tissue resected from humans with medial temporal lobe epilepsy.

Basic Circuitry

The perforant path is the major projection from the entorhinal cortex to the dentate gyrus of the hippocampus (See Figure 1) (Ramon y Cajal, 1893; Lorente de No, 1934). It plays a major role in delivering afferent information to the hippocampal formation (Lomo, 1971a; Witter, et al., 1989; Amaral and Insausti, 1990). The perforant path fibers terminate in the outer two-thirds of the dentate layer (Hjorth-Simonsen and Jeune, 1972; Hjorth-Simonsen, 1973; Steward, 1976; McNaughton and Barnes, 1977) where they make excitatory synapses onto the distal two-thirds of the granule cell dendrites (Lomo, 1971a). The remainder of the classic trisynaptic pathway consists of the unidirectional dentate granule cell output to area CA3 via mossy fibers followed by the unidirectional output of CA3 to area CA1 (Lorente de No, 1934; Andersen, et al., 1966b). This trisynaptic pathway is oriented in parallel lamellae perpendicular to the long axis of the hippocampus and has a high degree of topographic specificity (Andersen, et al., 1971; Hjorth-Simonsen and Jeune, 1972; Hjorth-Simonsen, 1973).

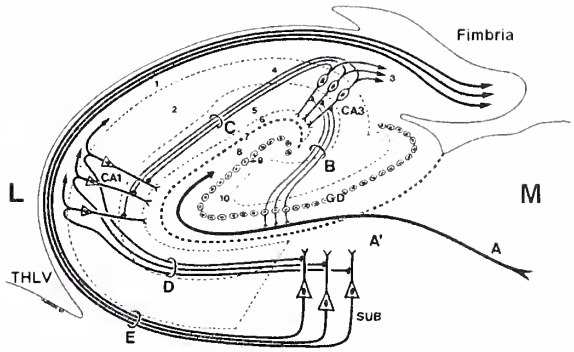

Figure 1: Diagram of the hippocampal formation as seen in transverse section perpendicular to the long axis of the hippocampus. Legend: The perforant path (A) innervates the dentate granule cells (GD) which send afferents to CA3 . CA3 in turn sends afferents to CA1 which then discharges to the subiculum. The subiculum sends output via the alveus (E) whose fibers gather in the fimbria. Abbreviations: M, medial; L, lateral; THLV, temporal horn of the lateral ventricle; GD, gyrus dentatus, SUB, subiculum. Adapted from (Duvernoy, 1988).

Orthodromic stimulation of the perforant path and subsequent firing of the granule cells initiates a feedback inhibition circuit via mossy fiber collaterals onto hilar interneurons (Andersen, et al., 1966a; Lomo, 1971a; Lomo, 1971b). (See Figure 2) The interneurons responsible for this feedback inhibitory activity have been identified as basket cells (Kandel, et al., 1961; Andersen, et al., 1964; Lomo, 1968; Matthews, et al., 1981). These cells lie at the hilar margin or immediately beneath it (Ribak, et al., 1982). In addition, indirect excitation of inhibitory cells by the perforant path input may elicit inhibition which is not recurrent in nature; this type of inhibition has been termed feedforward and may rely on activity dependent interneurons (Buzsaki and Eidelberg, 1982; Sloviter, 1991a).

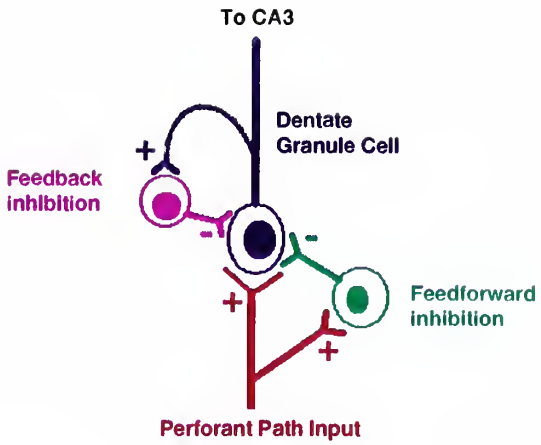

Figure 2: Simplified diagram illustrating feedback and feedforward inhibition. Direct excitation of inhibitory circuits by perforant path fibers (shown in red) may allow inhibition of single spikes via feedforward inhibition (shown in green). Output of the granule cells (shown in blue) may inhibit subsequent dentate granule cell activity via feedback inhibition (shown in magenta). Although these feedforward and feedback mechanisms are shown consisting of direct monosynaptic activation of inhibitory cells for simplicity, these circuits probably include other excitatory neurons (i.e., mossy cells) in a polysynaptic circuit.

Two distinct pathways have been identified between the entorhinal cortex and the dentate gyrus: the medial and lateral perforant pathways (Blackstad, 1958; Van Hoesen, et al., 1975; Krettek and Prince, 1977; Segal, 1977; Beckstead, 1978). The medial perforant path has been found to form synapses with the dentate dendritic tree in the outer one-third of the molecular layer, while the lateral perforant path terminates in the middle third (Hjorth-Simonsen, 1973). Although electrophysiological differences have been identified

between these pathways at high stimulus rates (McNaughton, 1980), these differences do not exist at lower stimulus frequencies (such as those used in this study) (Harris, et al., 1979).

The above antomical features allow a precise electrophysioloigcal study of the hippocampus through the utilization of known pathways to stimulate particluar populations of cells.

Dentate Granule Cell Stimulation

The field potentials evoked in the hippocampus by stimulation of the perforant pathway reflect several cell processes that occur simultaneously and therefore determine the shape of the observed waveform (Andersen, et al., 1966a). These include field excitatory post-synaptic potentials (fEPSPs), generated in the dendrites and action potentials, generated within or near the somal layers (Andersen, et al., 1966b; Lomo, 1971a). Overall, the typical positive-negative-positive waveform observed from dentate granule cell stimulation is thought to represent two summated processes: the extracellular EPSP and a superimposed population spike (PS) (See Figure 3) (Sloviter, 1991a). The triphasic appearance is simply produced by a PS occurring during the middle of the fEPSP. The depth of the PS is felt to be a measure of the number of neurons in a population generating action potentials (Lomo, 1971a).

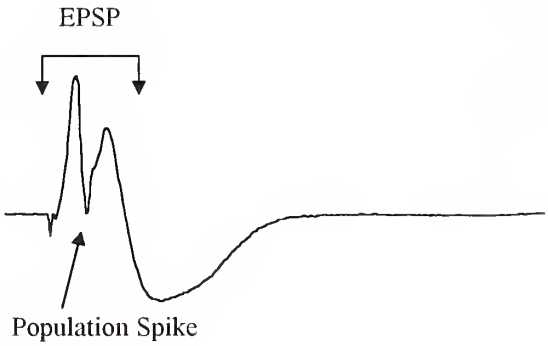

Figure 3: Typical waveform from dentate granule cells stimulated via the perforant path. The fEPSP is interrupted by the PS.

The paired-pulse paradigm of studying inhibition is one type of evoked response that may be applied to the investigation of epileptic tissue. It is based upon the premise that when the second pulse of a pair falls within the duration of a presumed recurrently generated inhibitory postsynaptic potential, the size of the population spike of the second pulse is diminished relative to the first (Barnes, 1979). This type of inhibition is called feedback inhibition and is quantified by taking the ratio of the amplitude of the population spike seen in response to the second stimulus ('PS(2)') to that elicited by the first stimulus ('PS(1)'). This same type of paradigm may be applied to the excitatory post synaptic potentials (EPSPs) as well.

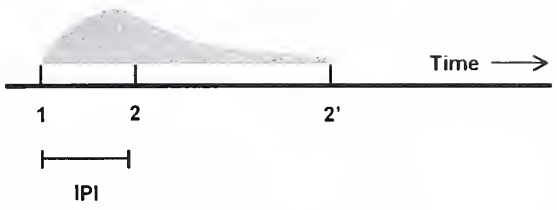

Figure 4: Diagram illustrating the premise of paired-pulse inhibition. The electrical stimulation at 1 (the conditioning stimulus) produces the theoretical inhibition represented in gray. A subsequent test stimulus at 2 would reveal an inhibited population spike because the inhibition is still present. The amount of time between the conditioning stimulus and the test stimulus is called the interpulse interval (IPI). Stimulation at a later time (2') would not show inhibition because it occurs past the duration of the inhibition.

In addition to these feedback mechanisms mentioned above, stimulation of the perforant path may elicit inhibition that is not recurrent and is feed forward in nature. Because it is felt that this feedforward inhibition relies upon activity-dependent interneurons, comparisons of both the PSs and EPSPs at different frequencies of stimulation may uncover evidence of this type of inhibition.

These paradigms are limited in their ability to examine precise mechanisms because stimulation may elicit several processes that can inhibit the test population spike (Bekenstein, et al., 1993), but, their utility lies in their ability to quantitate overall inhibition as it occurs in situ to a population of cells. Their use in this study allowed a quantification of inhibitory processes that occur in the human epileptic hippocampus.

Evidence for a Loss of Inhibition in Epilepsy

Histopathology of Human Hippocampus Resected For Intractable Epilepsy

The association of seizures and the lesion of hippocampal sclerosis has long been recognized (Sommer, 1880; Gastaut, 1953; Sano and Malamud, 1953). The hippocampi of medial temporal lobe epilepsy patients are characterized by cell loss in all areas including a mild cell loss in the dentate and a more marked loss in the dentate hilus (Mouritzen Dam, 1982; Houser, 1990; Kim, et al., 1990; Babb, et al., 1991; Masukawa, et al., 1992). The details of this loss from one study are presented in Table 1.

	Tumor	MTS
CA1	81.2%	34.8%
CA2	86.7%	50.7%
CA3	75.8%	39.8%
CA4	81.6%	39.5%
Dentate	80.7%	46.0%

Table 1: Percentage of cells present in the hippocampi of MTS and tumor related medial temporal lobe epilepsy patients expressed as a percentage the cell counts in a group of controls. Adapted from Kim, et al. 1990.

Reorganization of mossy fibers (sprouting) has also been demonstrated in the dentate gyrus of human temporal lobe epilepsy patients (Sutula, et al., 1988; de Lanerolle, et al., 1989; Houser, et al., 1990; Babb, et al., 1991; Masukawa, et al., 1992). These sprouted axons originate from the granule cell axons and have been shown to form extensive plexuses in the granule cell layer and molecular layer of the dentate gyrus, possibly forming an aberrant recurrent input (Isokawa, et al., 1993). Immunohistochemical techniques have also revealed sprouting of neuropeptide Y and somatostatin containing fibers in patients with MTS (de Lanerolle, et al., 1989; de Lanerolle, et al., 1992).

Numerous biochemical and immunohistochemical changes have also been elucidated. Interestingly, anatomical and histochemical studies of the hippocampus have shown that GABA (gamma-aminobutyric acid) containing cells are not lost in epileptic subjects and may even be preferentially preserved (Babb, et al., 1989). Within the dentate hilus, immunostaining of interneuron populations containing neuropeptide Y, somatostatin

and substance P have also been shown to be lost (de Lanerolle, et al., 1989; de Lanerolle, et al., 1992).

These changes described above provide clues to the mechanisms by which the loss of inhibition occurs and this study attempts to correlate electrophysiologic parameters of inhibition with the findings of atrophy both by MRI and by cell counts. Since GABA containing cells seem to be preserved, it is possible that changes in inhibition may be due to the loss of other cells in the hippocampus of these patients. This may result in the dysfunction of the GABAergic cells. In order to understand this dysfunction, the functions of GABA and its relationship to hippocampal electrophysiology need to be discussed.

Neurotransmitters

GABA is the primary inhibitory neurotransmitter in the central nervous system (Krnjevic, 1974). GABA acts on two pharmacologically distinct types of receptor, $GABA_A$ and $GABA_B$ (Ogata, 1990). Activation of $GABA_A$ receptors by synaptically released GABA increases membrane conductance, producing an early inhibitory postsynaptic potential (IPSP). In contrast, $GABA_B$ receptors are coupled through guanosine triphosphate (GTP)-binding proteins (Dutar and Nicoll, 1988b; Bowery, 1989; Ogata, 1990) and activation of these receptors increases membrane potassium conductance, producing a late IPSP (Dutar and Nicoll, 1988a). Granule cell firing is regulated by both feedback (Lomo, 1971b) and feedforward inhibition (Buzsaki and Eidelberg, 1982). Early feedback inhibition as evidenced through orthodromic paired-pulse depression in the rodent has been attributed to the $GABA_A$ receptor mediated inhibition (Andersen, et al., 1964; Matthews, et al., 1981; Alger and Nicoll, 1982; Thalman and Ayala, 1982; Tuff, et al., 1983). Late paired-pulse depression has been attributed to $GABA_B$ receptors on presynaptic perforant path terminals to decrease neurotransmitter release (Peer and McLennan, 1986). One recent study utilizing the $GABA_B$ receptor antagonist CGP-35348 indicated that $GABA_B$ receptors may have a role

in early paired-pulse inhibition as well (Brucato, et al., 1992). PS changes appear to be independent of EPSP changes suggesting that changes in the quantity of neurotransmitter released are not responsible for the inhibition of the PS, (Lomo, 1971b; Joy and Albertson, 1987; Krug, et al., 1990; Albertson, et al., 1991; Albertson, et al., 1992; Joy and Albertson, 1993) although other studies have indicated a role for these changes (Lomo, 1971b; Creager, et al., 1980).

In the hippocampal formation, GABAergic inhibition fades during repetitive stimulation (Ben Ari, et al., 1979; McCarren and Alger, 1985; Thompson and Gahwiler, 1992). For this reason, GABA is also thought to play a role in feed-forward inhibition (Alger and Nicoll, 1982). Mott et al. (1993) showed that $GABA_B$ autoreceptors are partially responsible for activity dependent disinhibition in the dentate gyrus.

It has been suggested that GABA disinhibition could provide a mechanism underlying the development of epilepsy (Meldrum, 1975; Wood, 1975; McDonald, et al., 1991). Using microdialysis techniques, extracellular GABA levels have been found to be significantly lower in the epileptogenic hippocampus of patients undergoing bilateral depth electrode studies for mesial temporal epilepsy (During and Spencer, 1993). Patients with tumor related epilepsy have also been shown to have decreased GABA and somatostatin containing neurons in adjacent hyperexcitable cortex (Haglund, et al., 1992). These findings of reductions in extracellular GABA in both MTS patients and patients with tumors raises issues regarding comparisons between the two groups. These electrophysiological findings in this study may be due to neurotransmitter changes such as those described above, although no attempt was made to study these directly.

MTS versus Tumors (tumors as a normal group)

There has been much discussion about what constitutes an adequate hippocampal control in human experiments of this type (Schwartzkroin, 1994). Such studies on human tissue are problematic because of the small quantity of tissue available, chronic exposure

to antiepileptic drugs, the potential for harboring other neurological processes and the difficulty in matching this tissue with appropriate controls (Bekenstein, et al., 1993). A potentially useful comparison group is those patients with mass lesions in the temporal lobe associated with their epilepsy. These masses are adjacent to, but not involving the hippocampus. They represent 9.5% to 22.5 % of temporal lobe epilepsy patients and form a distinct group (Cavanagh and Meyer, 1956; Currie, et al., 1971; Gastaut and Gastaut, 1976; Rassmussen, 1983; Rich, et al., 1985; Kuzniecky, et al., 1987; Bruton, 1988). Anatomical, immunohistochemical and electrophysiological data suggest that hippocampi resected from lesion-related temporal lobe epilepsy patients is more comparable to normal controls that tissue resected from patients with MTS (de Lanerolle, et al., 1989; Kim, et al., 1990; Fried, et al., 1992; Williamson, et al., 1993, Williamson, et al., 1990). This tissue has been previously used as a comparison population in studies of the human hippocampus (Williamson, et al., 1990; Sloviter, et al., 1991; Knowles, et al., 1992; Williamson and Spencer, 1994). However, it must be kept in mind that the group with structural lesions is not a normal control - these patients experience seizures that involve the hippocampus as well. For obvious reasons, the most appropriate control, normal human brain tissue, cannot ethically be used in studies such as this; this restriction may limit studies utilizing tumor related epilepsy controls because changes seen in both groups will not be revealed as significant differences in statistical analyses.

Animal Studies

Kindling

Kindling refers to a process whereby generalized electrographic and motor seizures can be produced by repeated electrical brain stimulation. Typically after a period of brief daily low intensity stimulation, the same stimulation that produced only brief afterdischarges prior to stimulation elicits a full generalized seizure. These seizures are not spontaneous and occur only in response to electrical stimulation. The changes in seizure

susceptibility are felt to reflect permanent changes in brain function (Goddard, et al., 1969). The kindling stimuli may be administered to any one of a number of sites including the amygdala, ipsilateral CA1, the hippocampal commissure, perforant path, or dentate hilus (Tuff, et al., 1983; King, et al., 1985; Oliver and Miller, 1985; de Jonge and Racine, 1987; Maru and Goddard, 1987; Zhao and Leung, 1992).

Several studies have looked at the effects of kindling on inhibition and have produced various results. Biochemical evidence exists for a disturbance of inhibition through the loss of GABA containing cells in the kindling model of epilepsy (Kamphuis, et al., 1986; Kapur, et al., 1989). Contrary to this, others have found elevated GABA release and elevated endogenous GABA levels in hippocampal slices from kindled rats (Leibowitz, et al., 1978). Several studies report decreased paired-pulse inhibition in the CA1 region of kindled animals (King, et al., 1985; Voskuyl and Albus, 1987; Kamphius, et al., 1988; Kapur, et al., 1989; Michelson, et al., 1989; Yamada and Bilkey, 1991; Kamphius, et al., 1992). In contrast, kindling results in enhanced paired pulse inhibition in the dentate gyrus (Tuff, et al., 1983; Oliver and Miller, 1985; de Jonge and Racine, 1987; Maru and Goddard, 1987; Stringer and Lothman, 1989; Robinson, 1991; Clusmann, et al., 1992; Zhao and Leung, 1992). These changes seen in the dentate gyrus may be stimulus intensity dependent. A significant reduction of paired-pulse inhibition has been found with medium stimulus intensities, while at higher stimulus intensities enhancement of inhibition was observed (Kamphius, et al., 1992). The authors hypothesized that the elevated number of benzodiazapene and GABA binding site found uniquely in the fascia dentata after kindling (Nobrega, et al., 1989; Nobrega, et al., 1990) may only be activated by strong stimuli and may underlie the observed enhanced inhibition. A potential shortcoming of the kindling model is that the spontaneous seizures seen in humans, do not occur (Bekenstein, et al., 1993).

Kainate-lesioning

Kainate is a potent excitatory neurotoxin when administered by intravenous, intracerebral or intraventricular routes (Ben Ari, 1985). It causes intense acute seizure activity followed by degeneration of hilar, CA3 and CA1 neurons (Nadler, et al., 1980). A state of abnormal excitability ensues (Franck and Schwartzkroin, 1985; Tauck and Nadler, 1985) and has been considered a model for temporal lobe epilepsy (Cavalheiro, et al., 1982; Ben Ari, 1985; Cronin and Dudek, 1988; Nakajima, et al., 1991). Spontaneous seizures have been shown to occur in this model (Cavalheiro, et al., 1982; Cronin and Dudek, 1988). Similar, but not identical neuropathological changes are seen in this model compared to those in human medial temporal lobe sclerosis (Lancaster and Wheal, 1982; Sloviter, 1987).

Decreased granule cell inhibition and increased excitability have been observed in this model (Sloviter and Damiano, 1981; Fisher and Alger, 1984; Cornish and Wheal, 1989; Sloviter, 1992). In addition, sprouting of the mossy fibers of the dentate granule cells has been shown to follow kainate lesions (Nadler, et al., 1980; Laurberg and Zimmer, 1981; Davenport, et al., 1990). These sprouted axons establish morphologically intact synapses in the inner molecular layer (Tauck and Nadler, 1985). Interestingly, excitatory changes were not found when the kainic acid lesion was associated with mossy fiber sprouting (Cronin, et al., 1992; Sloviter, 1992). However, when tonic inhibition was reduced by the $GABA_A$ receptor antagonist bicucilline in these animals with sprouting, hyperexcitablity compared to controls was observed (Cronin, et al., 1992). These studies give some indication that the mossy fiber sprouting observed following epilepsy-inducing lesions may be primarily inhibitory, rather than excitatory, and may functionally offset some of the induced damage. Conversely, other investigators have found evidence that these synapses may be functionally excitatory (Tauck and Nadler, 1985; Feldblum and Ackermann, 1987; Cronin and Dudek, 1988). A recent hypothesis has been offered that sprouting may cause both increased inhibition and increased excitability (Dudek, et al.,

1994). Overall, it appears that the functional effects of mossy fiber sprouting remain uncertain (Sutula, 1990). Correlations of the electrophysiological findings in this study with sprouting were examined through the use of stains for dynorphin and other neuropeptides in order to elucidate possible mechanisms by which the observed changes in inhibition occur.

Limbic status epilepticus

An important hypothesis relating to the limbic status epilepticus model is that of excitotoxic damage; this is based upon the supposition that if excitatory activity is of sufficient intensity for a sufficient duration, this excitatory input can destroy target neurons (Olney, et al., 1986). One version of this model relies upon a period of tightly clustered intermittent stimuli to the contralateral CA3 region which eventually produces a period of acute, nonconvulsive status epilepticus in both hippocampal formations which persist after cessation of the stimulus (Lothman, et al., 1990; VanLandingham and Lothman, 1991a; VanLandingham and Lothman, 1991b; Bekenstein, et al., 1993). Spontaneous seizures occur after this first stimulated seizure as a standard sequela (Lothman, et al., 1990) and a rapid deterioration of GABAergic inhibition ensues (Kapur and Lothamn, 1989). Morphologic changes similar to those seen in temporal lobe epilepsy are seen (Bertram, et al., 1990) and inhibition, as measured by the paired-pulse paradigm, was found to be decreased in this model (Bekenstein, et al., 1993).

A particularly relevant set of studies was performed by Sloviter (1991a, 1991b). In the first paper, paired pulse inhibition in the dentate gyrus was measured in normal rats (Sloviter, 1991a). At low stimulation frequency (0.1 Hz), inhibition of the response to the test stimulus by the conditioning stimulus was present at short interpulse intervals (20-40 msec). A frequency dependent increase in the strength and duration of this feedback inhibition was observed as the frequency of stimulation was increased from 0.1 Hz to 1.0 Hz. The conditioning stimulus was found to show some slight amount of inhibition as the

stimulus frequency was increased initially, followed by potentiation as the frequency was further increased. The low frequency elicited inhibition was felt to be of a feedback nature, while the initial effects of increasing stimulation rate on the conditioning spike were felt to occur via a feedforward mechanism. These effects were felt to be related to GABA function as this inhibition was blocked by the GABA antagonist bicucilline. At low stimulus intensities, the EPSP slopes were measured and found not to be effected by the administration of bicucilline suggesting that the same mechanisms responsible for the changes in the population spikes were not causing this effect via a GABA related effect on the EPSPs. The frequency dependent effects were hypothesized to occur by differences in hilar responsiveness at different stimulation rates as follows. At low frequency stimulation, there is minimal direct activation of hilar inhibitory cells (or of excitatory cells that subsequently innervate inhibitory cells). The output of the granule cells then feeds back into the hilar inhibitory circuit, thus eliciting the observed feedback inhibition of the second spike. As the frequency of stimulation was increased, feed-forward inhibition as defined by the inhibition generated by the direct afferent excitation of an inhibitory circuit, increases (Buzsaki, 1984). This may be due to the direct activation of basket cells (Amaral, 1978), axo-axonic inhibitory cells (Soriano and Frotscher, 1989) or hilar interneurons that activate inhibitory cells (Scharfman and Schwartzkroin, 1990). As frequency is further increased, frequency potentiation was felt to overcome this feed-forward inhibition, thus producing a large spike once again (Andersen and Lomo, 1967). It was felt by the author to be unclear why low frequency stimulation does not elicit strong feedforward inhibition, but it was speculated that increased frequency may increase inhibitory neuron discharge, increase depolarization-induced neurotransmitter release or may recruit additional inhibitory circuits.

An accompanying paper discussed changes in the dentate following the perforant path stimulation model of status epilepticus (Sloviter, 1991b). Following the period of induced status epilepticus by perforant path stimulation, paired pulse inhibition was found

to be markedly decreased. In addition, the frequency-dependent inhibition of the first spike was also lost. Frequently, multiple spikes were observed following stimulation especially at higher stimulation rates. These changes appeared to be permanent. GABA-immunoreactive cells were preserved following the stimulation (Sloviter, 1987; Sloviter, 1991b). Contrary to studies utilizing the kainate lesion model (Cronin, et al., 1992; Sloviter, 1992), the loss of inhibition appeared to be permanent and subsequent findings of mossy fiber sprouting were not associated with a restoration or enhancement of inhibition.

A major difference between human MTS and the limbic status epilepticus and kainate models is that CA1 pyramidal neurons were preserved, while these are lost in humans with MTS. The pattern of cell loss observed in these models appears to be similar to a much rarer lesion associated with epilepsy, "endfolium sclerosis" which has preservation of the CA1 neurons (Magerison and Corsellis, 1966; Bruton, 1988). Neuronal cell counts from patients with epilepsy have not demonstrated the presence of this lesion in any patients included in these studies (Mouritzen Dam, 1980; Babb and Brown, 1987; Kim, et al., 1990). One possible explanation for this difference in the limbic status epilepticus model is that the initial stimulation was carried out with the animal under urethane anesthesia. Other investigators using a similar model, in which the animal was not anesthetized, observed extensive CA1 damage (Rogers, et al., 1989).

The findings in this model led to the proposed "dormant basket cell" hypothesis. This hypothesis states that the loss of inhibition is due to loss of excitatory input to the main inhibitory interneurons of the dentate - the basket cells (Sloviter, 1991b). Careful intra-cellular investigations have been in support of this hypothesis (Bekenstein and Lothman, 1993).

The above animal models and their findings were instumental to the design of human studies such as this one. The paradigms developed and the results with their use have allowed a more focused approach to the electrophysiologic study of inhibition in populations of cells in the *human* hippocampus.

Human Studies

In-Vivo Studies

Rutecki et al. (1989) studied the hippocampi of temporal lobe epilepsy patients at the time of surgery. Hippocampal surface recordings were utilized while stimulating either the perforant path or the entorhinal cortical surface. The evoked responses did not consist of the previously described morphology from the dentate gyrus. Eleven of sixteen patients with the pathological findings of mesial temporal sclerosis manifested a simple waveform of a short latency positivity followed by a large negativity while four of six patients with non-infiltrating gangliogliomas (a low grade, possibly congenital tumor of neuronoglial origin) manifested a more complex waveform of multiple positive and negative components. In those patients with simple waveforms, no change in amplitude was seen as the stimulating frequency was varied from 1 to 10 Hz. Spontaneously occurring inter-ictal spikes in these patients were found to have a similar morphology to the evoked potentials.

Isokawa-Akesson (1989) studied nine patients undergoing evaluation for medial temporal lobe epilepsy by depth electrodes with the paired pulse paradigm. They found prolonged inhibition lasting up to 200 msec. One shortcoming of this study was that precise localization within the hippocampal formation of either the stimulating or the recording electrode was not possible. The results of this limited study suggested that inhibition is intact or even may be enhanced in the temporal lobe of human epileptic patients.

In Vitro Studies

Uruno et al. (1994) studied resected tissue taken from the hippocampi of temporal lobe epilepsy patients. Utilizing slice methodology, the tissue was classified into two groups by the number of population spikes evoked by orthodromic stimulation. Tissue with a single population spike was classified as "less excitable" while tissue with multiple population spikes was classified as "more excitable". The "more excitable" tissue

demonstrated less paired pulse inhibition than the "less excitable tissue" at an interpulse interval (IPI) of 20 msec.

Utilizing slice electorphysiology, Urban et al. (1993) found that the responses to perforant path stimulation in the dentate gyrus of patients with severely sclerotic hippocampi to consist of malformed, low amplitude field EPSP's and no clear evidence of synchronous population spikes. Recordings from individual cells indicated that the gross electrophysiological properties were normal, however, this study was performed with the small sample size of seven.

Isokawa et al. (1991) also found a loss of orthodromic paired-pulse depression in the dentate gyrus in slice preparations from human temporal lobe epilepsy patients. Utilizing intracellular techniques, fewer than half of the neurons manifested IPSPs following EPSPs. In those neurons without IPSPs, the EPSPs were prolonged to varying degrees. This late EPSP component was found to be NMDA receptor mediated. In addition, spike frequency accommodation was found to be intact and there was a lack of spontaneous or evoked burst discharges.

Experimental Means/Purpose of Study

Previous study of human epileptic cortex has consisted of extracellular recordings of spontaneous activity during the course of intracranial monitoring for the localization of the area of brain responsible for the generation of seizures (Babb, et al., 1984). Using a controlled input to elicit evoked responses provides a more scientific study of the electrophysiological properties. The in vitro slice preparation has permitted further in depth scientific study of this tissue. Classic studies of the hippocampus indicated that the slice preparation was particularly well suited for this type of study because of its lamellar structure (Andersen, et al., 1971; Hjorth-Simonsen and Jeune, 1972; Hjorth-Simonsen, 1973), but other studies have indicated substantial interlammelar connections (Lorente de No, 1934; Swanson and Cowan, 1977; Laurberg and Sorensen, 1981). The role of these

connections has yet to be defined. Differences in the manifestations of epileptic properties between tissue in-vivo and in-vitro have led to concern about the limitations of the slice preparation technique (Schwartzkroin, et al., 1983). Furthermore, this type of study is not available until after the tissue has been resected, limiting its potential usefulness in the decision-making process for surgery for epilepsy. One further drawback, particularly in utilizing this technique in humans is that the tissue may experience a period of ischemia during the course of resection which could possibly alter the subsequent findings.

At the time of surgery, the hippocampus is revealed in-situ with most of its connections intact. This presents a unique opportunity for the electrophysiological study of the hippocampus prior to its resection. It is obvious from the above that the animal models are not in agreement with regard to the loss of inhibition in the dentate gyrus. Furthermore, the one in-vivo human study indicated a gain in inhibition, while the human in-vitro studies indicated a loss of inhibition. Thus, questions remain regarding the applicability of the animal models to the human state and between the possible differences of human in-vivo and in-vitro study of the dentate gyrus. The purpose of this study was to quantify the status of the inhibitory circuits of the dentate gyrus of the hippocampus as they appear in-situ in the human with medial temporal lobe epilepsy, eliminating issues regarding the possible loss of substantial interlammelar connections. The waveforms elicited from the dentate gyrus by perforant path stimulation were analyzed and inhibition in the dentate gyrus was quantified. This was achieved by 1) using the paired-pulse paradigm to quantify feedback inhibition and by 2) observing changes elicited by changing stimulation frequency to examine feedforward inhibition and frequency related potentiation. This data was used in a comparison of hippocampi between patients with MTS and patients with tumor related epilepsy. Other clinical and scientific findings for these patients were also correlated with these findings in an effort to further define the differences in electrophysiological findings between these groups.

Materials and Methods

Patients

The patients studied were selected from a consecutive series of patients from July 1993 to July 1994 who underwent evaluation by the Yale Epilepsy Surgery Program and were recommended for standard anteromedial temporal resection for medically refractory epilepsy. The decision in recommending surgery for any individual patient included analysis of numerous data sources including history, interictal and ictal-EEG monitoring, MRI including hippocampal volumes, positron-emission tomography (PET), single photon emission computed tomography (SPECT), neuropsychological evaluation, intracarotid amytal testing and in some instances invasive monitoring techniques. The procedure that follows was approved by the Human Investigations Committee of Yale School of Medicine and signed written consent was obtained from each patient prior to operation. The experimental procedure was carried out during the course of the clinically indicated surgery and the patients remained on their current antiepileptic drug regimen until the time of surgery. The patients were grouped upon their final pathological report as read by the neuropathologist. These two groups consisted of patients with mesial temporal lobe sclerosis (MTS) and patients with lesions.

Anesthesia

The end-tidal level of isoflurane was adjusted to 0.25% and adequate time was given for the patient to clear any nitrous oxide that had been administered. Of note, benzodiazepines, barbiturates and propofol were avoided in these cases because of their known alteration of electrophysiologic properties of brain tissue. During the time of recordings, the patients were primarily managed with the above anesthetic and constant rate fentanyl drip anesthesia.

Surgical Exposure

The surgery was carried out as has been previously described (Spencer, et al., 1984b). Briefly, after intubation and the initiation of general anesthesia, the scalp was reflected and bone removal was carried out. The temporal pole and anterior 3-3.5 cm of the middle and inferior temporal gyri were removed to a depth of approximately 3 cm. The temporal horn of the lateral ventricle was entered and the incision was continued anteriorly and medially across the anterior fibers of the temporal stem. Retractors were then placed revealing the hippocampus in the opened ventricle.

Electrode Implantation

A bipolar stainless steel stimulating electrode was placed under direct visualization through the parahippocampus 1-2 mm posterior to the pes-body junction so as to place the tip in the vicinity of the perforant path. (labeled 'stimulate' in Figure 5).

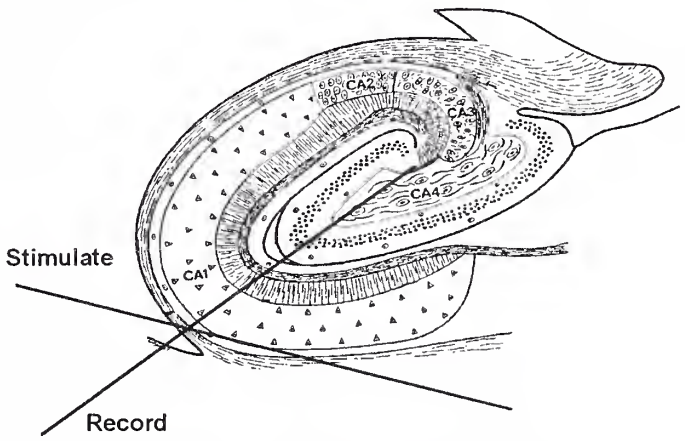

Figure 5: Diagram of the hippocampus showing the trajectories of the stimulating and recording electrodes

This stimulating electrode consisted of two exposed portions of stainless steel 0.5 mm in length, 0.1 mm in diameter, 2 mm apart. A recording electrode was placed at the pes-body junction at a different angle so as to place the tip of the electrode through the dentate granule cell layer (labeled 'record' in Figure 5). This recording electrode consisted of eight contacts, 0.5 mm in length, 0.1 mm in diameter and 1 mm apart along the length of the electrode. In the initial twelve patients, these electrodes were inserted without any direct feedback. In the following twelve patients, the electrodes were placed during continuous 1 Hz stimulation and visualization of elicited waveforms. Whenever possible, the placement was altered in such a way to provide maximal amplitude EPSP and PS

responses. In addition, an attempt was made to cross the dentate gyrus at the middle of the electrode so that some contacts appeared proximal and some distal to the waveform interpreted as representing the granule dentate cell layer. This was done so that the voltage reversal (flip) could be observed (See Figure 10). In addition, a four contact stainless steel surface recording strip was placed under the entorhinal cortex in a longitudinal fashion. When space was adequate, another recording strip was placed so as to cover the surface of the hippocampus with the anterior most contacts over the amygdala. Apart from the stimulating electrode, all of the above mentioned contacts were utilized in a monopolar fashion with the ground needles attached to the muscle/scalp flap.

Stimulation and Data Acquisition

After placement of these electrodes, stimuli were administered via the stimulating electrode in order to establish a threshold for observable evoked potentials. This was achieved by using a Grass S88 stimulator (Grass Instrument Company, MA), which was triggered by a personal computer to administer 100 μsec square constant current pulses at 1 Hz. After establishing the threshold for response, the current for the stimulation experiment was set at the smaller of twice the threshold current or 10 mA. This ceiling current level was established within the requirements of the Human Investigations Committee in order to ensure the safety of the experiment.

After a five minute interval, a paired-pulse experiment at a fixed interstimulus interval (ISI) was carried out using the electrode placed in the perforant path. A pair of pulses was administered every 5 seconds (0.2 Hz). Ten trials of pulses at interpulse intervals (IPI's) of 0 (representing a single pulse), 20, 40, 60, 100 and 200 msec were administered in a random, biphasic fashion. The evoked responses were digitally recorded after 2-5K amplification with a bandpass filter of 0.3-1000 Hz. 1024 point epochs were digitized at a sampling rate of 2000 Hz.

Following the paired pulse experiment, single stimuli were administered at varying frequencies: 0.1, 0.2, 0.5, 1, 2, and 3 Hz. The evoked responses for ten trials were digitized as above after an initial two stimuli were administered at each frequency to eliminate frequency transition related phenomena.

Lesioning

After stimulation, electrolytic lesions were created between the two most distal contacts of each electrode so as to provide a means of verification of the location of the probes. After the hippocampus was removed the section that was thought to contain the lesion was divided into 450 micron (10^{-6} meters) continuous vibratome sections and each was wet mounted and examined under the microscope in an attempt to locate the lesion and thus identify the precise area being stimulated and recorded.

Data Analysis

The ten responses to each stimulus condition were averaged for each of the channels recorded. A narrow bandwidth digital notch filter was applied as needed to eliminate line noise. For the paired-pulse experiment, the averaged response to a single pulse at 0.2 Hz was subtracted from the epoch recorded for each pair in an attempt to minimize the interference of the first waveform on the

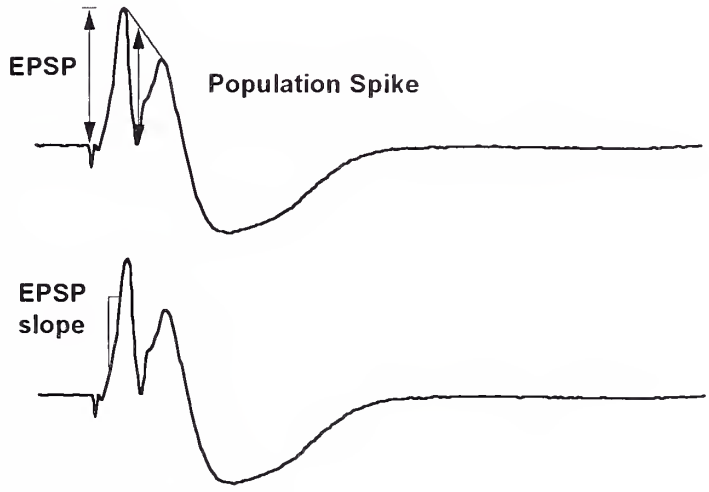

Figure 6: Methods used for waveform measurements. The EPSP amplitude was measured from the baseline to the maximum EPSP height. The population spike amplitude was measured from a straight line connecting the interrupted peaks of the EPSP to the maximal negativity. The EPSP slope was measured as the slope between $1/e$ and $2/e$ of the initial EPSP height.

visualization of the second waveform in each pair. The baseline to peak (b-p) amplitude of the EPSP was measured as the difference between the baseline (taken as the averaged voltage for the period 10 msec prior to the stimulus) and the maximum point of the response. The slope of the initial EPSP segment was measured as defined by the slope of a line connecting two points, which were selected as representing $1/e$ and $2/e$ (36.8% and 73.6%) of the initial EPSP amplitude. The ratio of the measurement taken after the second stimulus of each pair to the measurement taken for the single pulse was then calculated (i.e., the b-p for the response to the second pulse at 100 msec divided by the b-p response to the single pulse). These ratios will be referred to as EPSP(2)/EPSP(1) or EPSPslope(2)/EPSPslope(1). For those cases in which a PS was also observed, the amplitude of the PS was measured as the distance from the projected straight line connecting the two peaks of the interrupted EPSP to the maximal negativity of the PS and the ratio was calculated in a similar way. This ratio will be referred to as PS(2)/PS(1). The ratios of the PS to EPSP amplitude and slope were also calculated in an effort to elucidate changes in PS that were independent of EPSP amplitude changes (Maru, et al., 1989). These will be referred to as [PS/EPSP](2)/[PS/EPSP](1) and [PS/EPSPslope](2)/[PS/EPSPslope](1). For each individual patient, the measurements for the channel which contained either the maximal amplitude EPSP or, if available, the channel immediately prior to the phase reversal were used in the group analysis. Excluded from the group data were any individual waveforms for any particular IPI where the individual components of the waveform were not obvious and measurable.

Other Variables

Pathological Diagnosis

The patients were categorized into the lesion related group or the MTS group based upon the diagnosis given in the final pathology report issued by the Division of

Neuropathology. Their examination included portions of the hippocampus, parahippocampus, amygdala and lateral neocortex.

Hippocampal Volumes

For the details of this procedure, please see McCarthy and Luby (1994). Briefly, preoperatively, a 3-D volume set of coronal MRI images (SPGR 3 mm slices, TR/TE = 25/5, FOV 16) was obtained. These images were then reformatted into oblique images perpendicular to the long axis of the hippocampus and adjustments were made for head rotation if needed. The hippocampus was carefully outlined on each of the five images starting 3 mm anterior to the superior colliculus. The volume of the hippocampus was taken as the sum of the outlined areas of each of these. For convenience, in this study the volumes are reported in summed pixel areas rather than converting this value to a true volume.

Hippocampal Cell Counts

This procedure was carried out by one investigator (J. Kim) as delineated by Kim et al. (1990, 1995) Briefly, a 2 mm slice sectioned perpendicular to the long axis of the hippocampus was selected from the mid or mid-posterior portion of the *en-bloc* resected specimen. The slice was fixed in 10% buffered formalin, dehydrated and parrafin embedded. Six micron sections were then stained with hematoxylin and eosin. For each patient five or more consecutive sections were counted by two investigators and the counts combined. Each of the regions CA1, CA2, CA3, CA4 and the dentate granule cell layer were counted separately. This was accomplished by counting the neuronal nuclei in each unit area of a 200 μm x 400 μm rectangle for regions CA1-CA4 and a 50 μm x 100 μm rectangle for the dentate granule cell layer. The entire CA fields and granule cell layer were covered with multiple continuous unit areas through the ocular grid as counting was being performed. The neuronal counts obtained were adjusted using Abercrombie's formula (Abercrombie, 1946) utilizing 8 μm for the nuclear diameter of pyramidal neurons

and 6 μm for the granule cell layer neurons. The neuronal density was expressed as the mean neuronal number/mm^3.

For the purposes of this study, these counts were converted into the percent cell loss compared to controls by using the published average neuronal densities calculated for 22 non-epileptic autopsy controls (age and sex matched to the Yale Epilepsy Surgery Program patient population) using the above method (Kim, et al., 1995). In addition, utilizing the published standard errors, the cell loss for each patient in each hippocampal subfield was designated as significant or not significant based upon whether the neuronal density was more than two standard deviations from the mean.

Immunocytochemistry

All immunohistochemical studies were performed by the same investigator (N. de Lanerolle) in accordance with the published procedure (de Lanerolle, et al., 1992). Briefly, the hippocampus was vibratome sectioned into 500 micron blocks and fixed in a buffered picric acid/paraformaldehyde mixture for 1 hour. This was followed by immersion in 5% acreolein in 0.1 M phosphate buffer, pH 7.4 for approximately 3 hours. This tissue was then immunostained with antibodies for neuropeptide Y (NPY), somatostatin (SS) or dynorphin (DYN) using the peroxidase-antiperoxidase or the avidin-biotin complex method. The stained sections were observed under the microscope and for each specimen the presence or absence of sprouted *fibers* containing the above substances was noted.

Because staining for each of the above antibodies (NPY, SS and DYN) was not available for all of the patients, the results were pooled in the following manner. Evidence of sprouting on any stain was simply designated as the presence of sprouting, while the absence of sprouting on all stains was designated as the absence of sprouting. In no cases in this series was there any contradictory evidence of sprouting of one type in the absence of the other.

Computer Programs

Stimulation Program

Visual Basic 3.0™ was chosen as the programming environment, in part because of the availability of dynamic link libraries for this language for the stimulation board (PC-TIO 10, National Instruments, Ohio). The stimulation program was designed to work with the data acquisition program MIP (© 1990, Tony Andrignolo) which was utilized for the digitization of the data in these experiments. The program was run on a 486-33DX PC in a monitoring room immediately adjacent to the operating room. A separate 486-25DX was utilized for the MIP program. Briefly, during the paired-pulse experiment, the user indicates the frequency of stimulation and the time interval between pairs (IPIs) for up to eight different IPIs. In addition, the number of trials is also indicated. The program then randomizes all of the pairs, so as to reduce the effects of any slow processes that might occur during the stimulation on any particular set of IPIs. During the stimulation, a signal is sent to the Grass 88 stimulator and to the MIP program simultaneously to initiate the data acquisition. After the set IPI, an additional signal is sent to the stimulator to fire the second pulse of the pair. A similar paradigm was used for the frequency experiments, except only single pulses were used and the frequencies were randomized. In order to eliminate any possible

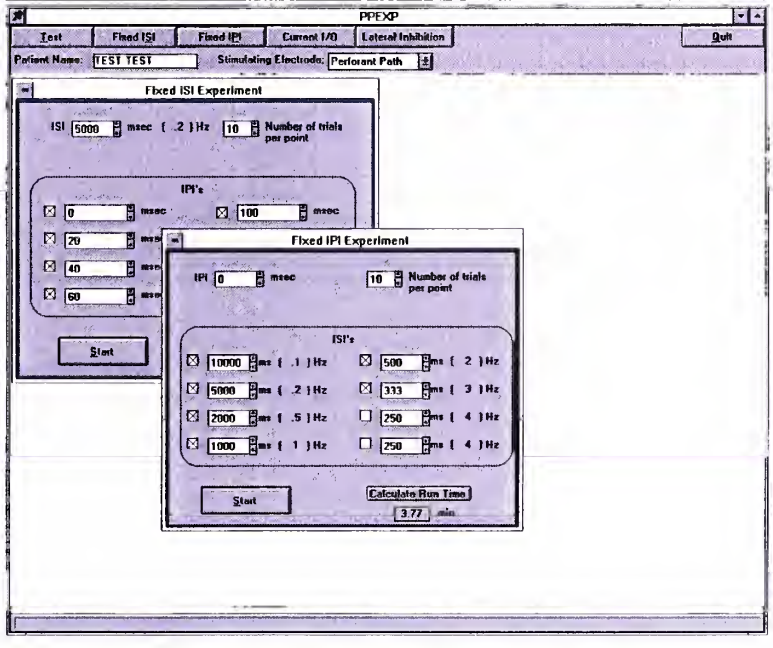

Figure 7: An example of the interface of the program written to perform the stimulation.

changes that might take place during the transition from one frequency to the next , a five second pause was provided between the change of frequencies. This was followed by the administration of two stimuli at the given frequency prior to the initiation of the acquisition at each frequency. An example of the program interface is shown in Figure 7.

Real Time Waveform Display

After the experience in the initial twelve patients, it was felt that direct visualization of the waveforms during electrode placement could improve the chances of recording population spikes by providing direct feedback. This was accomplished by writing a Visual Basic™ program to digitize and display the recorded potentials along the length of the recording electrode in real-time. The output from this program was displayed on a monitor within the operating room during the electrode insertion. An example of the user interface for this program is shown in Figure 8.

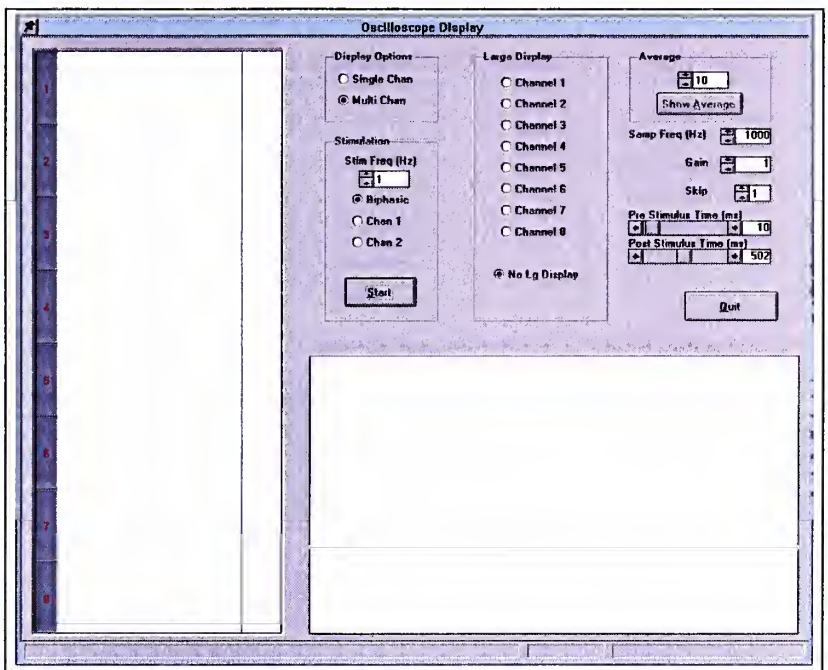

Figure 8: An example of the user interface of the real-time waveform display program.

Data Analysis

A Visual Basic™ program was written to perform the waveform analysis. This program processed the entire data set for each experiment. The waveform subtractions, filtering and measurements were carried out by this program. The equation for the notch filter that was utilized is given as:

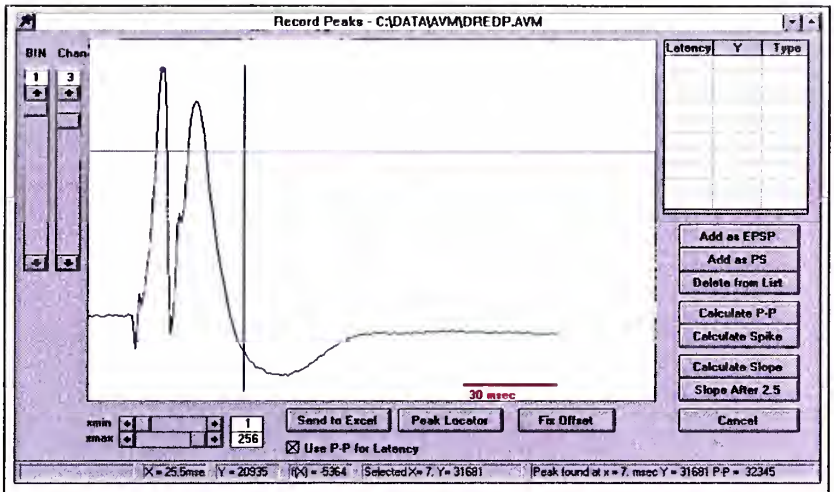

Figure 9: An example of a portion of the user interface of the program written for waveform analysis.

$$H(z) = \frac{(z - e^{j\theta_c})(z - e^{-j\theta_c})}{(z - R_p e^{j\theta_c})(z - R_p e^{-j\theta_c})},$$

where Rp in the above equation represents the bandwidth (set to 0.95 for these experiments) (Strum and Kirk, 1989). This was applied via numerical methods in multiple passes both forwards and backwards to reduce ringing artifacts in any one direction. This program interacted directly with either Microsoft Excel 5.0ä via dynamic data exchange (DDE) or later directly with Microsoft Access 2.0ä to store the measurements made. In addition, a paper plotting routine was included to produce hard copy output of the waveforms. An example of waveform measurement portion of this program is given in Figure 9.

Statistical Procedures

For pairwise comparisons, nominal data was tested using the chi-squared or Fisher's exact test, while continuous data was tested using Student's t-test. Non-parametric measures (Mann-Whitney-U and Spearman rank-order coefficients) were used

for all analyses involving the cell count data as this data is known not to meet continuity criteria for parametric testing. The level of significance was set to 0.05, two tailed for all tests. All of the experimental ratio data was analyzed using the SAS Generalized Linear Models Procedure (VMS SAS 5.10, SAS Institute Inc., NC). A two-way ANOVA for repeated measures was carried out using a nested design (Keppel, 1973). The nested variable TNT (this variable represents the pathological diagnosis, lesion or MTS, i.e. TNT = 1 for lesion patients, while TNT = 2 for MTS patients) and the IPI (five levels representing the five different IPIs used) were considered fixed independent variables. The PS, EPSP, EPSP slope, PS/EPSP and PS/EPSP slope ratios were treated as dependent variables individually. For each set, the interaction term (i.e. TNT x IPI) and each main effect (TNT and IPI) was tested for significance using the F-ratio. The interaction term is the critical term for assessing a difference in each group over the various IPIs, while each main effect individually tests for significance independent of the other variable (i.e. TNT tests for differences independent of IPI). This same procedure was carried out for the five different frequencies used in the frequency experiment. All other nominal variables used in ANOVAs were analyzed in a similar manner.

Statement of Collaboration

All of the work in the previous delineation of the Material and Methods section was performed by the primary author with the following exceptions:

1.) Selection of patients as surgical candidates for medically intractable epilepsy was carried out by the Yale Epilepsy Surgery Program. Clinical data, MRI scans and hippocampal volumes were obtained as a part of this process.

2.) Anesthesia was performed by the Department of Anesthesia of Yale School of Medicine in accordance with standard practices for epilepsy surgery.

3.) The surgical exposure and actual physical placement of the electrodes was performed by Dennis D. Spencer, M. D., Professor and Chief of the Division of Neurosurgery.

4.) All neuronal densities and counts were performed by Jung H. Kim, M. D., Associate Professor of the Section of Neuropathology. Neuropathological reports regarding the tissue were generated by the Section of Neuropathology.

5.) All immunohistochemical staining and evaluation was performed by Nihal C. de Lanerolle, D. Phil., Associate Professor of the Division of Neurosurgery.

The author was present at the clinical decision making meetings regarding surgical candidacy for all patients. Selection of patients for inclusion in the study was carried out by the author in conjunction with Dennis D. Spencer, M.D. The first author was present at each surgery and aided in guidance of the placement of the electrodes and performed the data collection. All parameters for stimulation intensities and frequencies were established by the author in conjunction with Dennis D. Spencer M.D. and Gregory McCarthy, Ph.D. All programs listed above for real-time display, stimulation paradigms, and data analysis the exception of the 'MIP' program for data acquisition were written by the author. Lesion creation and identification of lesions in the resected specimen was carried out by

the author. All statistical analysis was performed by the author. This study was carried out as a portion of a larger program-project for the study of entorhinal-hippocampal interaction in medial temporal lobe epilepsy patients.

RESULTS

Patients

One patient whose waveforms were recorded was excluded from the study because no firm pathological diagnosis could be established and the case was done with the patient awake, whereas all the other cases were done under isoflurane-fentanyl anesthesia as described in the Methods section.

A summary of the characteristics of the remaining 23 patients and the differences between the lesion group and the MTS group is given in Table 3. Seventeen patients were placed in the MTS category, while six were found to have mass lesions (See Table 2). The hippocampal volumetric data, cell count data and immunohistochemistry for sprouting were not available for all patients and this is reflected in the table. The patients in these two groups differed significantly in several variables: the number of years of recurrent seizures prior to surgery ($p = 0.04$), the hippocampal volume ratios and absolute hippocampal volumes ($p = 0.0020$ and $p = 0.0050$, respectively), and the neuronal density in CA1 ($p = 0.0178$) and in the dentate gyrus ($p = 0.0343$). Of note is that there is no significant difference in the medication regimens of the two groups. The CA4 neuronal density and the presence or absence of sprouting did not differ significantly between the two groups but these measures were only available for three of the patients in the lesion group.

Pathological Diagnosis	Number
Low-Grade Astrocytoma	2
Cavernous Hemangioma	2
Oligodendroglioma	1
Dysembryoplastic Neuroepithelial Tumor	1

Table 2: Pathological Diagnosis in the Six Lesion Patients

	MTS	Tumor	P
Number	17	6	
Age	31.74 (12.42)	25.99 (14.87)	0.36
Male:Female	7:10	3:3	0.94
Handedness L:R	3:14	0:6	0.097
Age Onset of Recurrent Seizures	6.07 (6.87)	13.45 (15.99)	0.13
Yrs of Szs Prior to Sx	25.67 (14.32)	12.55 (3.27)	**0.04**
Side of Surgery L:R	11:6	4:2	0.73
Hippocampal ratio	-0.121 (0.029)	-0.013 (0.0048)	**0.0020**
Hippocampal volume	826 (52.7)	1264 (83.4)	**0.0050**
On Carbamazepine	11	4	1.00
On Dilantin	7	2	1.00
On Valproate	5	0	0.272
On Phenobarbital	1	1	0.462
On Mysoline	3	0	0.539
On Other Medications	3	0	0.539
CA4 density (cells/mm^3)	7826 (562)	2715 (1380)	0.0719
CA3 density (cells/mm^3)	14656 (954)	(7814) 5368	0.1066
CA2 density (cells/mm^3)	15399 (1082)	10735 (2426)	0.0890
CA1 density (cells/mm^3)	11210 (664)	3520 (1296)	**0.0178**
Dentate density (cells/mm^3)	252607 (12068)	165637 (26982)	**0.0343**
Sprouting (Y:N)	11:4	0:3	1.00
Seizure Outcome (Success:Failure)	15:2	6:0	1.00

Table 3: Summary of patient characteristics. Bold figures indicate statistical significance. For binary variables, the number shown is the number of patients from each group. For continuous variables, the number shown is the mean, while the standard error of the mean is shown in parentheses. P is the probability of rejecting the null hypothesis. For counts, P reflects the probability calculated using Fisher's Exact Test (two-tailed), while for continuous variables, P reflects the probability calculated using Student's T-Test (two-tailed).

Results of Single Stimuli

In the initial eleven patients, population spikes were not observed. After the implementation of a program to directly visualize the waveforms during the surgery, population spikes were visualized in eleven of twelve patients. This was accomplished by repeated adjustment of the stimulating and recording electrodes until the typical dentate granule cell waveform was observed. A typical pattern across the multicontact electrode is shown in Figure 10.

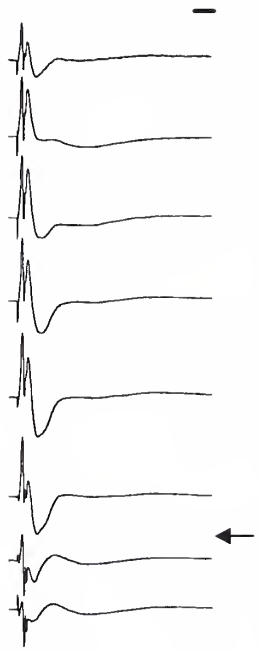

Figure 10: An example of the typical response along the length of the recording electrode to single stimuli. The orientation is distal to proximal from top to bottom. The arrow indicates the transitional flip which occurs as the electrode passes though the dentate granule cell layer. The recordings below this may represent dendritic potentials in the molecular layer or potentials generated in CA1. The time bar at the top is 20 msec in length.

Paired Pulse Inhibition

The results from a typical experiment utilizing the paired-pulse paradigm is shown in Figure 11. This particular example is taken from a patient with a medial temporal lobe tumor and demonstrates intact inhibition at short IPIs which recovers by the 200 msec IPI. The measurements from such

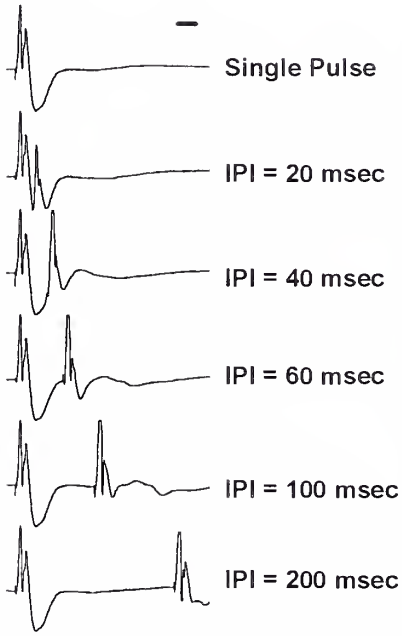

Figure 11: An example of the waveforms recorded from one channel during the paired-pulse experiment. During data analysis, the single pulse tracing was subtracted from the paired-pulse tracings so that measurements could be made which were not distorted by the potentials generated during the conditioning stimulus. The bar represents 20 msec.

experiments were compiled and analyzed by ANOVA to test differences in inhibition between the lesion and MTS patients over the course of the different IPIs. For each independent variable the interaction of the pathological state (denoted TNT) and the IPI were tested. This interaction effect is denoted as 'TNT x IPI' in the Table 4. The interaction term is the critical term in testing for differences in the dependent variable over time (IPI) between the two groups. The main effects of TNT and IPI were tested individually as well. Testing of the main effects of each of these factors reveals differences in the dependent variable for each factor, which are independent of the other factor (i.e. testing the main effect of factor A looks at the differences in the dependent variable as grouped by factor A, regardless of factor B). The results are shown in Table 4.

Dependent Variable	Test Variable	F-ratio	P-value
PS ratio	TNT	0.07	0.7949
	IPI	0.48	0.7497
	TNT x IPI	5.25	**0.0018**
EPSP ratio	TNT	1.67	0.2097
	IPI	12.89	0.0148
	TNT x IPI	0.55	0.7016
EPSP slope ratio	TNT	0.09	0.7658
	IPI	30.46	0.0030
	TNT x IPI	0.03	0.9985

Table 4: ANOVA results for the paired-pulse experiment. The factor 'TNT' is a class level variable which represents the pathological state: MTS or lesion. For each dependent variable the main effects of TNT and IPI and the interaction effect of TNT with IPI were tested. (See Statistical Procedures, p. 28) A significant interaction was found for the population spike ratios ($p = 0.0018$). The main effect of IPI was also significant for the EPSP ratio and EPSP slope ratio data.

A significant difference was found between the lesion patients and the MTS patients for the population spike ratio data. These results are shown graphically in Figure 12. The lesion group showed early inhibition at an IPI of 20 msec, followed by recovery at the longer IPIs. The MTS patients showed a smaller amount of inhibition than the lesion patients at an IPI of 20 msec. Furthermore, this inhibition did not recover during the length of IPIs sampled. These results indicate a loss of feedback inhibition in the MTS patients at an IPI of 20 msec. In addition, a low-level state of inhibition, which did not

vary with IPI and did not recover over the time course of IPIs tested was observed in the MTS patients.

The same type of analysis was carried out for the EPSP amplitude ratio (hereafter referred to simply as the EPSP ratio). The results of the ANOVA are also included in Table 4. No significant interaction was found between the pathological diagnosis and the IPI for the EPSP ratios or the EPSP slope ratios. These results are shown in Figure 13.

Although there is no significant difference between the two groups in the interaction term ($p = 0.7016$), there is clearly an effect of IPI ($p = 0.0148$). Both groups demonstrate that the EPSP height is initially inhibited at 20 msec followed by recovery.

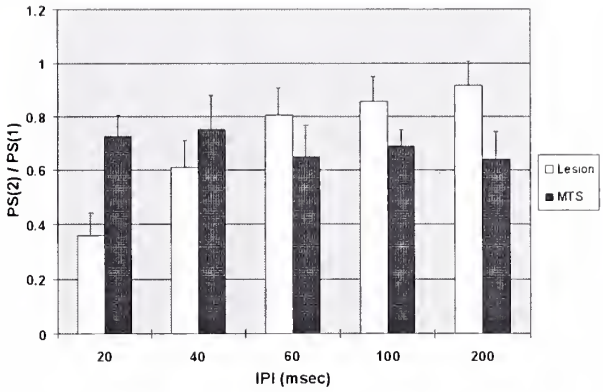

Figure 12: Population spike ratio results for the paired-pulse experiment for the lesion patients compared to the MTS patients. ANOVA showed a significant interaction of pathological state with IPI ($p = 0.0018$). A loss of inhibition for the MTS patients is demonstrated at 20 msec. This early inhibition recovers in the lesion patients while the low-level inhibition in the MTS patients does not. Error bars indicate the standard error of the mean.

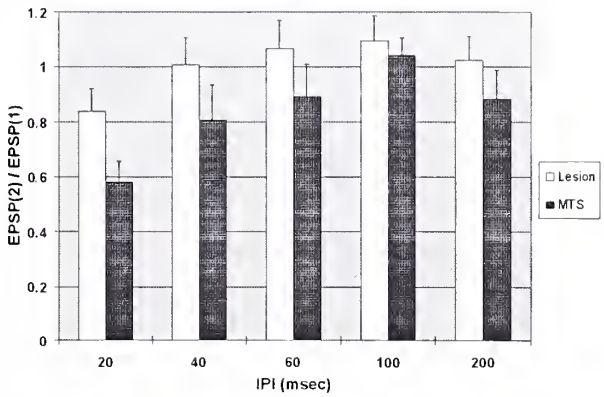

Figure 13: EPSP ratio results for the paired-pulse experiment. There was no significant interaction effect of IPI with pathological state.

The same analysis was repeated for the EPSP slopes. The results of the ANOVA are also found in Table 4 and shown graphically in Figure 14. No significant interaction was found for IPI versus pathology ($p = 0.9985$) and again there was significant effect of IPI ($p = 0.0030$).

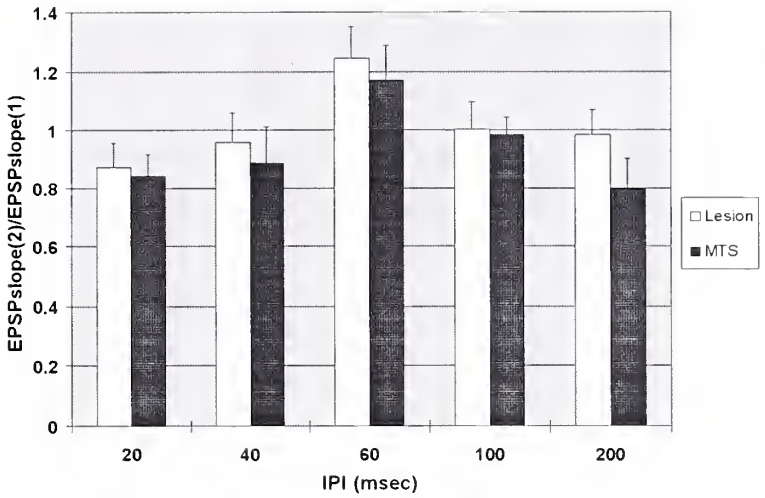

Figure 14: EPSP slope ratio results for the paired-pulse experiment. ANOVA showed no significant interaction of IPI with pathological state.

The above results indicated a significant change in the EPSP amplitude and EPSP slope which varied with IPI. The possibility that these effects may influence the PS ratio results was investigated further. Previous animal studies have raised concerns regarding this phenomenon (Maru, et al., 1989; Krug, et al., 1990; Joy and Albertson, 1993). In an attempt to study this further, the ratios of the PS to the EPSP and EPSP slope were calculated for the single stimulus data and compared between the two groups. The results are shown in Table 6. For the single stimuli, there is a significant difference in the ratio of the population spike to the EPSP or EPSP slope between the lesion and MTS groups ($p = 0.0128$ and $p = 0.0448$, respectively). A greater amplitude of population spike was generated for the same EPSP or EPSP slope in the lesion patients compared to the MTS patients.

Dependent Variable	Test Variable	Mean	t(t-test)	P-value
$PS_{ss}/EPSP_{ss}$	Lesion	1.30	2.9960	**0.0128**
	MTS	0.60		
$PS_{ss}/EPSPslope_{ss}$	Lesion	4.92	2.2643	**0.0448**
	MTS	1.91		

Table 6: Comparison of the population spike to EPSP and EPSP slope ratios ($PS_{ss}/EPSP_{ss}$ and $PS_{ss}/EPSPslope_{ss}$) for the single stimulus data. The subscript 'ss' was used to denote that these ratios are calculated for the single stimulus data. Both variables are significantly different between groups.

Although this analysis indicates a significant difference between the groups, the utilization of the population spike *ratios* reduces the effect of these differences as each parameter (PS, EPSP or EPSP slope) is compared to the single stimulus data in the same subject in performing this calculation (i.e., intersubject differences in the PSs are minimized because the results of the single stimuli are used in the denominator in each ratio). These effects could still affect the population spike data if the relationship of the population spike to the EPSP or EPSP slope varies with IPI. In order to investigate this further, the population spike ratio was divided by the EPSP ratio or EPSP slope ratio at each IPI to elucidate the changes in the population spike ratio which were independent of the changes in EPSP or EPSP slope ratios (Maru, et al., 1989). The results of the ANOVA are shown in Table 5. This revealed a significant interaction of IPI with pathology for the PS/EPSP ratio ($p = 0.0008$). These results are shown graphically in and Figure 15.

Dependent Variable	Test Variable	F-ratio	P-value
PS/EPSP ratio	TNT	0.05	0.8212
	IPI	0.14	0.9560
	TNT x IPI	5.96	**0.0008**
PS/EPSPsl ratio	TNT	0.61	0.4496
	IPI	0.37	0.8194
	TNT x IPI	2.56	0.0545

Table 5: ANOVA results for the PS to EPSP and EPSP slope ratios.

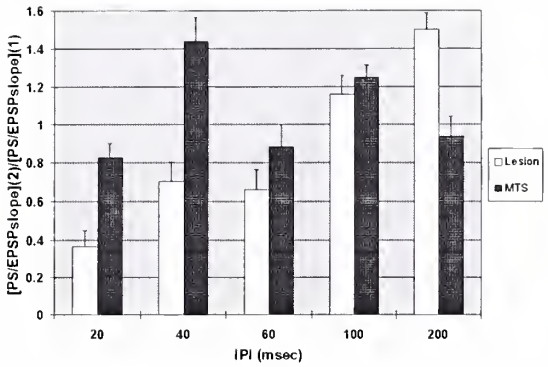

Figure 15: PS/EPSP slope results for the paired pulse experiment. No significant interaction between IPI and the pathological diagnosis was found.

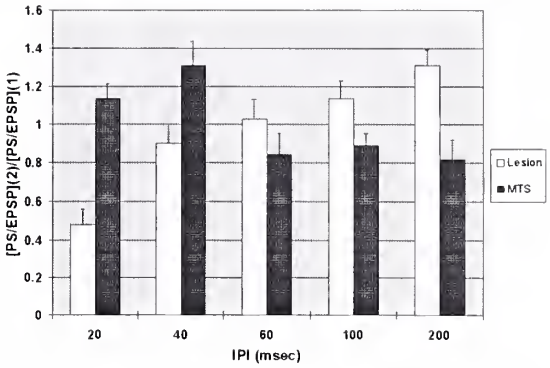

Figure 16: PS/EPSP ratio results for the paired-pulse experiment. A significant interaction between IPI and the pathological diagnosis was found ($p = 0.008$)

Rate Dependent Inhibition

The results for the frequency experiment were analyzed in a similar manner. The PS ratios, EPSP ratios and EPSP slope ratios were compared between the lesion patients and the MTS patients. The results of the ANOVA are shown in Table 7. This again revealed a significant interaction of IPI with the pathological diagnosis for the PS ratio data. The results of these experiments are shown graphically in Figure 17, Figure 18 and Figure 19. The MTS patients demonstrated a progressive attenuation of the PS as frequency was increased compared to the lesion patients.

Dependent Variable	Test Variable	F-ratio	P-value
PS ratio	TNT	0.54	0.4875
	IPI	1.20	0.4319
	TNT x IPI	3.32	**0.0240**
EPSP ratio	TNT	0.16	0.6973
	IPI	1.91	0.2727
	TNT x IPI	0.21	0.9296
EPSP slope ratio	TNT	0.21	0.6504
	IPI	0.71	0.6245
	TNT x IPI	1.52	0.2083

Table 7: ANOVA results for the frequency experiment. A significant interaction was found between IPI and the pathological diagnosis for the PS ratio data ($p = 0.0240$).

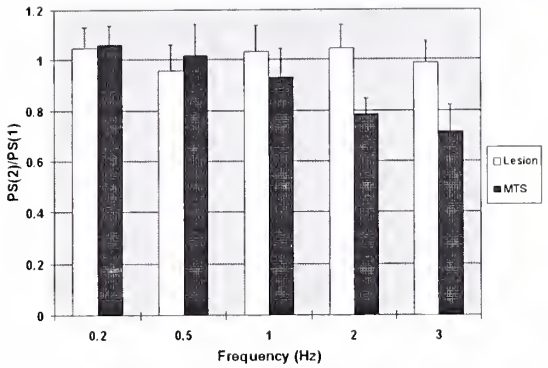

Figure 17: Population spike ratio results for the frequency experiment. A significant interaction between IPI and the pathological diagnosis was found ($p = 0.0240$).

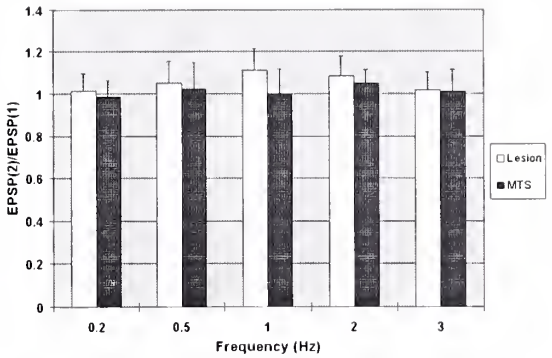

Figure 18: EPSP ratio results for the frequency experiment. No significant interaction was found.

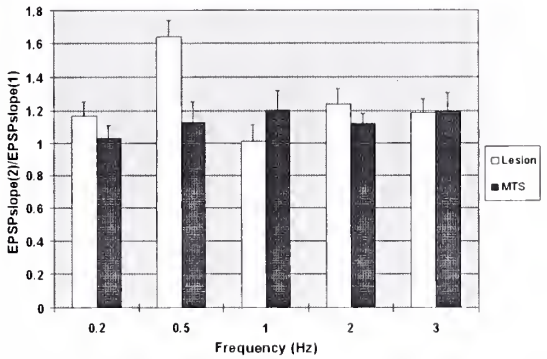

Figure 19: EPSP slope ratio results for the frequency experiment. No significant interaction was found.

Because the results for the single stimulus and paired-pulse experiment indicated that the ratio of the PS to the EPSP and EPSP slope may clarify significant findings, this was repeated for the frequency experiment. The results of the ANOVA are shown in Table 8. These indicate a significant interaction of IPI with the pathological diagnosis for both the PS/EPSP and PS/EPSP slope ratios. These results are shown graphically in Figure 20 and Figure 21.

Dependent Variable	Test Variable	F-ratio	P-value
PS/EPSP ratio	TNT	0.51	0.5019
	IPI	0.33	0.8486
	TNT x IPI	5.56	**0.0026**
PS/EPSPsl ratio	TNT	0.22	0.6580
	IPI	0.84	0.5652
	TNT x IPI	3.53	**0.0210**

Table 8: ANOVA results for the PS/EPSP and PS/EPSP slope ratios for the frequency experiment. Significant interactions of IPI with the pathological diagnosis are revealed for both variables (p = 0.0026 and p = 0.0210).

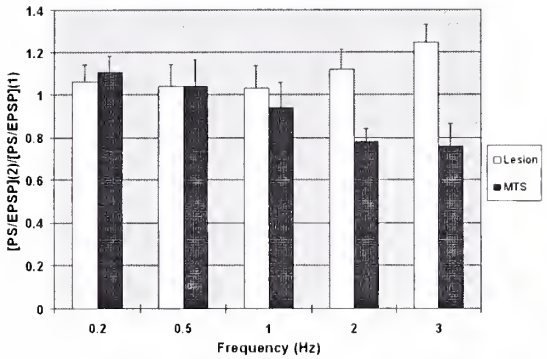

Figure 20: PS/EPSP ratio results for the frequency experiment. A significant interaction of IPI with the pathological diagnosis was found (p = 0.0026).

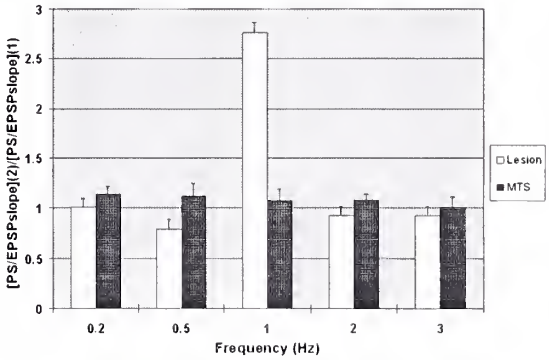

Figure 21: PS/EPSP slope results for the frequency experiment. A significant interaction of IPI with the pathological diagnosis was found (p = 0.0210).

These results suggest that the observed attenuation of the PS spike is independent of the changes in EPSP height. This also revealed a potentiation of the PS ratio as frequency was increased. The seemingly anomalous result for the PS/EPSP slope data at 1 Hz will be discussed in the Discussion on page 60..

Correlations with Hippocampal Volumetrics

Hippocampal volumetric measurements were available for 23 of the 24 patients. The hippocampal ratio was taken as the "diseased" side (the side operated upon) minus the "normal" side divided by the sum of the volumes for both hippocampi. In order to test these measures in an analysis of variance as was done for the previous data, the hippocampal ratios were ranked from first to last and split into upper and lower halves and then used in the ANOVA. The results of this for the paired-pulse experiment and the frequency experiment are shown in Table 9. No significant interactions of the dependent variables were revealed in this analysis.

		Paired-Pulse Experiment		Frequency Experiment	
Dependent Variable	Test Variable	F-ratio	P-value	F-ratio	P-value
PS	HR half	1.03	0.3332	5.18	0.0631
	IPI	0.51	0.7335	2.19	0.2329
	HR half x IPI	0.81	0.5300	1.78	0.1659
EPSP	HR half	0.34	0.5652	0.75	0.6052
	IPI	6.36	0.0503	0.41	0.7989
	HR half x IPI	2.1	0.0883	5.18	0.0631
EPSP Slope	HR half	0.17	0.6877	0.63	0.4394
	IPI	0.84	0.5672	0.57	0.6989
	HR half x IPI	1.12	0.3532	1.00	0.4170
PS/EPSP ratio	HR Half	0.14	0.7176	2.80	0.1553
	IPI	0.48	0.7547	2.68	0.1815
	HR Half x IPI	1.01	0.4144	1.10	0.3852
PS/EPSPsl ratio	HR Half	0.91	0.3617	1.51	0.2741
	IPI	1.23	0.4217	0.85	0.5619
	HR Half x IPI	0.96	0.4434	0.49	0.7435

Table 9: ANOVA results for the paired-pulse and frequency experiments for the patients grouped by 'HR half'. The variable 'HR half' represents whether the patient was in the upper half or lower half of the ranked hippocampal ratios. No significant interactions were seen between IPI and the 'HR half' for any of the dependent variables in either experiment.

The volumetric ratio procedure described provides some normalization for variations in hippocampal size between subjects, but it was felt that this might obscure the relationship with the electrophysiologic data The same methodology mentioned above was applied for the hippocampal volumes on the operated side. The patients were ranked according to hippocampal volume and divided in half. The results for the paired-pulse experiment and the frequency experiment are shown in Table 10. The variable 'HV half' indicates whether the patient was in the upper or lower half. This revealed a significant interaction of IPI with the upper or lower hippocampal volume half for the PS ratio data in the paired-pulse experiment ($p = 0.0001$). These results are shown graphically in Figure 22.

		Paired-Pulse Experiment		Frequency Experiment	
Dependent Variable	Test Variable	F-ratio	P-value	F-ratio	P-value
PS	HV half	2.55	0.1384	0.05	0.8244
	IPI	0.12	0.9679	5.26	0.0684
	HV half x IPI	7.62	**0.0001**	1.01	0.4191
EPSP	HV half	0.22	0.6471	2.51	0.1355
	IPI	8.99	0.0280	0.83	0.5679
	HV half x IPI	1.25	0.2973	0.67	0.6126
EPSP Slope	HV half	2.36	0.1399	0.02	0.8904
	IPI	1.60	0.3299	0.60	0.6829
	HV half x IPI	1.02	0.4009	0.78	0.5422
PS/EPSP ratio	HV Half	0.06	0.8116	0.00	0.9621
	IPI	0.30	0.8676	2.57	0.1911
	HV Half x IPI	2.43	0.0640	1.38	0.2691
PS/EPSPsl ratio	HV Half	0.02	0.8917	0.24	0.6421
	IPI	0.42	0.7887	0.71	0.6257
	HV Half x IPI	1.77	0.1558	1.24	0.3205

Table 10: ANOVA results for both experiments for the data grouped by 'HV half.' The variable 'HV half' denotes whether the patient was in the upper or lower half of hippocampal volumes. A significant interaction of IPI with 'HV half' was observed for the PS ratio data in the paired-pulse experiment. ($p = 0.0001$).

Patients with larger hippocampi had more inhibition at short IPIs than patients with more atrophied hippocampi. These differences became less at longer IPI's.

To further elucidate this interaction, a linear regression was carried out at each IPI for the PS ratio versus the hippocampal volume. The results of this are shown in Table 11. This revealed a significant correlation of the PS ratio data to the hippocampal volume at an IPI of 20 msec (r = 0.819, p = 0.0096). This relationship is shown graphically in Figure 23.

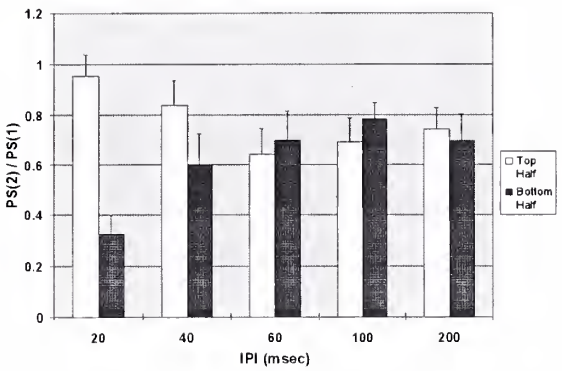

Figure 22: PS ratio results for the paired pulse experiment. A significant interaction of IPI with upper vs. lower hippocampal half was observed (p = 0.0001).

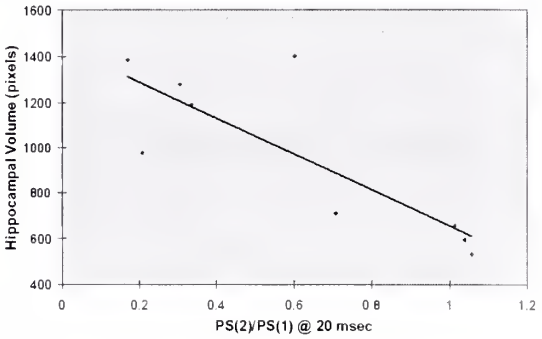

Figure 23: Results of the linear regression for the PS ratio at 20 msec versus the hippocampal volume. There is a significant correlation between the PS ratio at 20 msec and the hippocampal volume (r = 0.819, p = 0.0096)

IPI	R-Squared	F-ratio	P	Slope
20	0.6712	14.288	**0.0069**	-0.00085
40	0.0895	0.786	0.4010	-0.887
60	0.0410	0.342	0.5745	0.0002
100	0.1235	1.268	0.2892	0.0002
200	0.0017	0.015	0.9040	0.00002

Table 11: Linear regression results for the PS ratio in the paired-pulse experiment versus the hippocampal volume.

Correlations with Neuronal Densities

Neuronal cell densities were available in twenty of the twenty-four patients. Using the known average and standard deviation for the control population, (Kim, et al., 1995) these data were converted into z-scores. A significance level of $z = 2$ was set and then the patients were divided into groups with or without significant loss for each area for which the densities were available (dentate gyrus (DG), CA1, CA2, CA3 and CA4). These groups were then tested by ANOVA for interactions of the presence or absence of significant cell loss with IPI for each of the dependent variables. The results for the paired-pulse experiment and frequency experiments are shown in Table 12. A significant association was found for the EPSP ratios in the paired-pulse experiment versus the neuronal densities in the dentate gyrus and CA4 ($p = 0.0007$ and 0.0089, respectively). This is shown graphically in Figure 24 and Figure 25. The EPSP ratio is seen to increase with increasing frequency in patients without significant DG or CA4 loss. Spearman rank order coefficients were calculated for the EPSP ratio versus the DG cell density and the CA4 cell density at each IPI. The results of this are shown in Table 13.

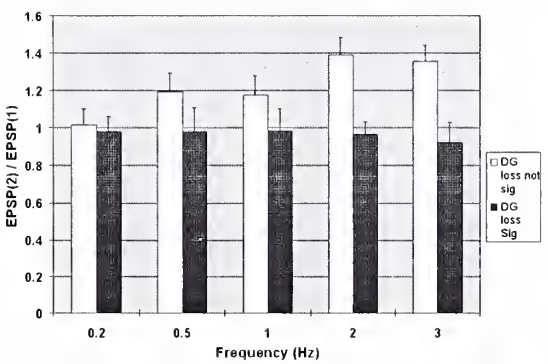

Figure 24: EPSP ratio results for the frequency experiment where the groups are divided by the presence or absence of significant dentate neuronal loss ($p = 0.007$).

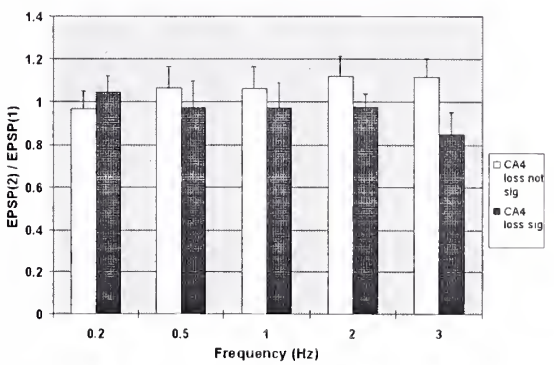

Figure 25: EPSP ratio results for the frequency experiment where the groups are divided by the presence or absence of significant CA4 neuronal loss ($p = 0.0089$).

		Paired-Pulse Experiment		Frequency Experiment	
Dependent Variable	Test Variable	F-ratio	P-value	F-ratio	P-value
PS	DG sig x IPI	0.91	0.4705	0.41	0.7971
PS	CA4 sig x IPI	0.33	0.8538	0.91	0.4705
PS	CA3 sig x IPI	1.05	0.3949	0.87	0.4929
PS	CA2 sig x IPI	1.01	0.4168	0.20	0.9346
PS	CA1 sig x IPI	0.45	0.7733	0.20	0.9346
EPSP	DG sig x IPI	0.31	0.8725	5.54	**0.0007**
EPSP	CA4 sig x IPI	0.70	0.5952	3.73	**0.0089**
EPSP	CA3 sig x IPI	0.40	0.8116	0.10	0.9820
EPSP	CA2 sig x IPI	1.18	0.3245	0.20	0.9392
EPSP	CA1 sig x IPI	0.68	0.6105	0.35	0.8432
EPSP Slope	DG sig x IPI	1.69	0.1592	1.59	0.1883
EPSP Slope	CA4 sig x IPI	1.96	0.1081	0.32	0.8866
EPSP Slope	CA3 sig x IPI	1.10	0.3535	0.36	0.8332
EPSP Slope	CA2 sig x IPI	0.78	0.5389	0.23	0.9211
EPSP Slope	CA1 sig x IPI	1.33	0.2661	0.20	0.9384
PS/EPSP ratio	DG sig x IPI	0.99	0.4264	0.64	0.6365
PS/EPSP ratio	CA4 sig x IPI	1.55	0.2082	0.27	0.8952
PS/EPSP ratio	CA3 sig x IPI	1.00	0.4201	0.08	0.9880
PS/EPSP ratio	CA2 sig x IPI	0.32	0.8640	0.77	0.5553
PS/EPSP ratio	CA1 sig x IPI	0.37	0.8293	0.77	0.5553
PS/EPSPsl ratio	DG sig x IPI	0.50	0.7367	0.92	0.4708
PS/EPSPsl ratio	CA4 sig x IPI	0.59	0.6690	1.30	0.2989
PS/EPSPsl ratio	CA3 sig x IPI	0.43	0.7833	0.62	0.6502
PS/EPSPsl ratio	CA2 sig x IPI	0.41	0.7990	0.32	0.8593
PS/EPSPsl ratio	CA1 sig x IPI	0.51	0.7265	0.32	0.8593

Table 12: ANOVA results for the neuronal cell density experiments for the paired-pulse and frequency experiments grouped by the presence or absence of significant cell loss. The variable for each area (e.g. DG sig = signifcant dentate gyrus) is a binary variable representing the presence or absence of significant cell loss. Significant interactions between IPI and significant DG and CA4 cell loss were observed for the EPSP ratio in the frequency experiment ($p = 0.007$ and $p = 0.0089$).

	Dentate Density		CA4 Density	
Freq	Correlation Coefficient	P	Correlation Coefficient	P
0.2	0.309	0.2380	-0.171	0.519
0.5	0.770	**0.0000**	0.276	0.292
1	0.550	**0.0266**	0.65	0.533
2	0.710	**0.0019**	0.268	0.308
3	0.632	**0.0084**	0.368	0.156

Table 13: Spearman Rank order coefficient results for the EPSP ratio in the frequency experiment. Significant correlations were seen only for the dentate neuronal density.

The correlation analysis revealed significant correlations at frequencies of 0.5 ($p = 0.000$), 1.0 ($p = 0.0266$), 2.0 ($p = 0.0019$) and 3.0 Hz ($p = 0.0084$) with the dentate granule cell densities. These results are shown graphically in Figure 26, Figure 27, Figure 28, and Figure 29. The EPSP ratio in the frequency experiment is seen to increase with increasing dentate granule cell density.

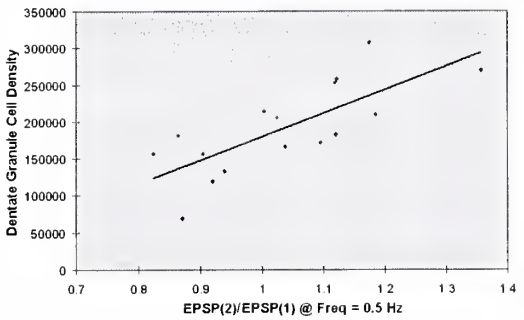

Figure 26: Graph of dentate neuronal density versus the EPSP ratio for the frequency experiment at 0.5 Hz. Spearman correlation coefficient = 0.770, p = 0.000.

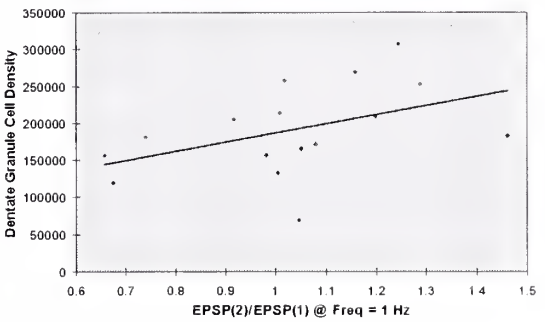

Figure 27: Graph of dentate neuronal density versus the EPSP ratio for the frequency experiment at 1.0 Hz. Spearman correlation coefficient = 0.550, p= 0.226.

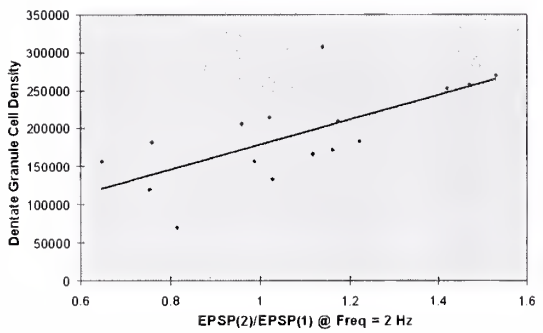

Figure 28: Graph of the dentate neuronal density versus the EPSP ratio for the frequency experiment at 2 Hz. Spearman correlation coefficient = 0.710, p = 0.0019.

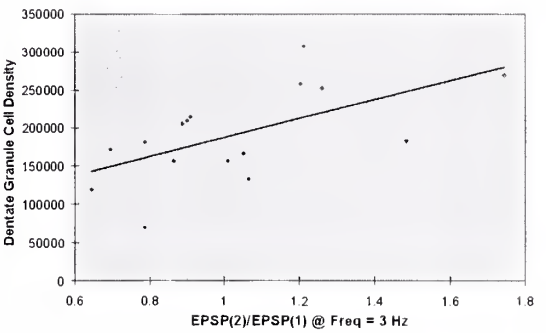

Figure 29: Graph of the dentate neuronal density versus the EPSP ratio for the frequency experiment at 3 Hz. Spearman correlation coefficient = 0.632, p =0.0084

Correlations with Sprouting

Immunohistochemical results for the presence or absence of sprouting were available for 18 patients (In the other five patients staining was not performed due to inadequate tissue, errors in fixing, etc.). The interaction of the presence or absence of sprouting with IPI was tested for each of the dependent variables. The results are shown in Table 14.

		Paired-Pulse Experiment		Frequency Experiment	
Dependent Variable	Test Variable	F-ratio	P-value	F-ratio	P-value
PS	Sprouting x IPI	0.80	0.5385	1.56	0.2159
EPSP	Sprouting x IPI	0.18	0.9472	4.77	**0.0026**
EPSP Slope	Sprouting x IPI	0.77	0.5515	1.99	0.1105
PS/EPSP ratio	Sprouting x IPI	1.50	0.2356	2.17	0.1091
PS/EPSPsl ratio	Sprouting x IPI	0.22	0.9145	0.32	0.8614

Table 14: ANOVA results for both experiments for the presence or absence of sprouting. A significant interaction of IPI with sprouting for the EPSP amplitude was revealed in the frequency experiment ($p = 0.0026$).

This revealed a significant interaction for the EPSP ratio in the frequency experiment. This is shown graphically in Figure 30.

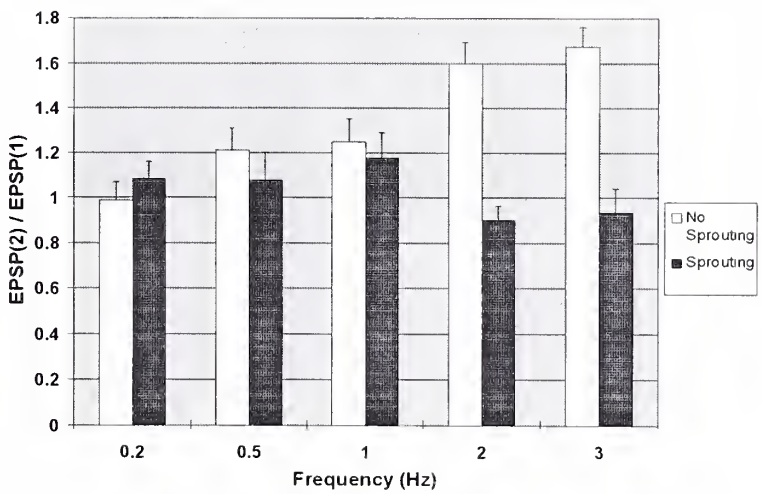

Figure 30: Results for the EPSP ratio in the frequency experiment grouped by the presence or absence of sprouting.

Correlation with Clinical Variables

The clinical variable identified from the patient characteristics that was significantly different between the lesion and MTS patients was the number of years of seizures prior to coming to surgery. The patients were ranked according to this variable and then split into upper and lower halves. The interaction of this variable with IPI was then tested by ANOVA for each of the dependent variables. The results are shown in Table 15.

Significant interactions were found for the PS ratio and the PS/EPSP ratio for the paired-pulse experiment. This is shown graphically in Figure 31 and Figure 32.

		Paired-Pulse Experiment		Frequency Experiment	
Dependent Variable	Test Variable	F-ratio	P-value	F-ratio	P-value
PS	MedYrsSzs x IPI	7.89	**0.0001**	2.24	0.0897
EPSP	MedYrsSzs x IPI	0.5	0.7391	0.88	0.4839
EPSP Slope	MedYrsSzs x IPI	0.24	0.9127	1.12	0.3567
PS/EPSP ratio	MedYrsSzs x IPI	2.78	**0.0407**	2.41	0.0775
PS/EPSPsl ratio	MedYrsSzs x IPI	1.84	0.1415	1.11	0.377

Table 15: ANOVA results for both experiments grouped by median number of years of seizures (MedYrsSzs). Significant effects were observed for the PS ratio and PS/EPSP ratio in the paired-pulse experiment (p = 0.0001 and p = 0.0407).

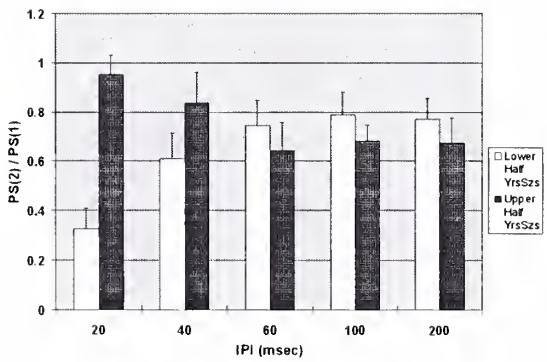

Figure 31: Results for the PS ratio in the paired pulse experiment grouped by the number of years of seizures. A significant interaction between IPI and the number of years of seizures was found (p = 0.001)

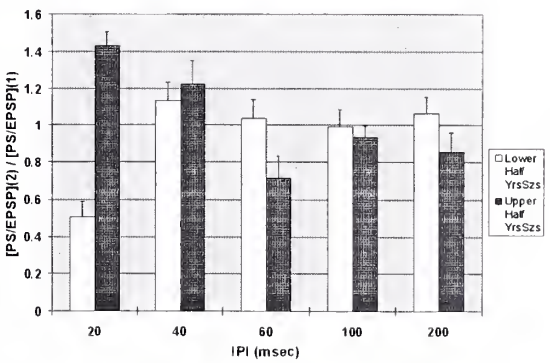

Figure 32: Results for the PS/EPSP ratio in the paired-pulse experiment grouped by the number of years of seizures. A significant interaction between IPI and the number of years of seizures was found (p = 0.0407)

The results for the PS ratio data were tested by linear regression with the number of seizures at each IPI. The results are shown in Table 16. These results show that a correlation exists only for an IPI of 20 msec. This is shown graphically in Figure 33.

IPI	R-Squared	F-ratio	P	Slope
20	0.7788	24.643	**0.0016**	0.018
40	0.5112	7.322	0.0304	0.011
60	0.0161	0.114	0.7452	0.002
100	0.0539	0.399	0.5478	-0.003
200	0.0299	0.216	0.6563	-0.002

Table 16: Regression results for the PS ratio data in the paired pulse experiment versus the number of years of seizures. A significant correlation is revealed between the number of years of seizures and the PS ratio at an IPI of 20 msec.

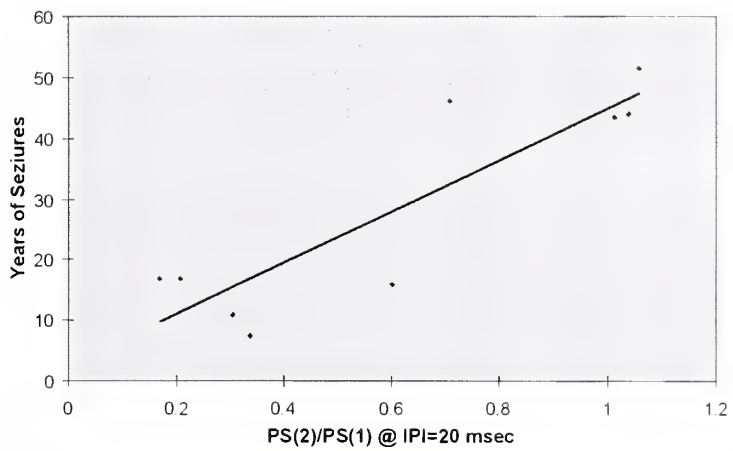

Figure 33: Graph of the number of years of seizures versus the PS ratio for the paired-pulse experiment at IPI = 20 msec.

Lesioning

Definite evidence of the lesions created during surgery were found in the sectioned tissue of only six patients. However, the location of the lesions corresponded roughly with the observed waveforms. In those which crossed the dentate layer, a definite phase reversal of the waveform was observed, while in those that only came to the edge of the dentate layer, only the distal most contacts revealed the typical waveform (See Figure 34).

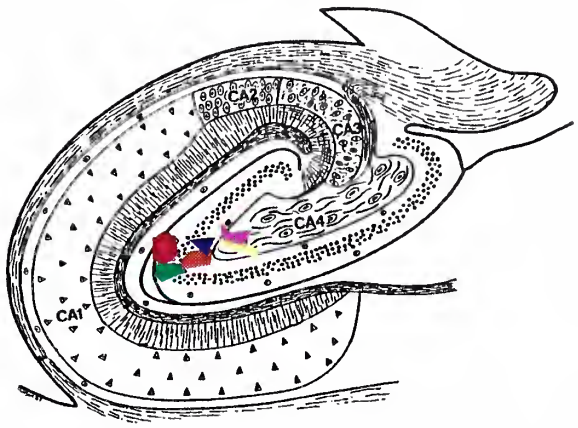

Figure 34: Summary of lesion locations.

DISCUSSION

Major findings

This study has shown that a number of parameters of hippocampal inhibition can be measured at the time of surgery for medial temporal lobe epilepsy and are positively correlated with a number of clinical and histological variables. These include:

1) A loss of feedback inhibition as measured by the PS ratio in the paired-pulse experiment in MTS patients compared to lesion patients. This was further seen to be independent of EPSP changes.
2) A loss of feedback inhibition as measured by the PS ratio in the paired-pulse experiment in patients with larger hippocampi compared to patients with more atrophied hippocampi and a direct correlation of the loss of feedback inhibition at an IPI of 20 msec with the hippocampal volume.
3) A direct correlation of the loss of feedback inhibition measured by the PS with the number of years of seizures.
4) A loss of feedforward inhibition as measured by the PS ratio in the frequency experiment at 1 Hz in both MTS and lesion patients.
5) Frequency related potentiation of the PS in lesion patients compared to frequency related attenuation in MTS patients at frequencies above 1 Hz. This was also shown to be independent of EPSP changes.
6) Frequency related potentiation of the EPSP in patients with non-significant dentate granule cell and CA4 loss and sprouting compared to frequency related attenuation in patients with significant loss in these areas. The dentate granule cell density showed a positive correlation with the EPSP ratio at stimuli of 0.5, 1 ,2 and 3 Hz.
7) A decrease in PS/EPSP and PS/EPSP slope ratios in MTS patients compared to lesion patients for single stimuli.

Descriptive findings

None of the waveforms recorded indicated the presence of multiple population spikes. Previous investigations have observed this phenomenon in the in-vitro human slice preparation from epileptic patients with stimulation of the perforant path (Masukawa, et al., 1989; Williamson, et al., 1990; Masukawa, et al., 1991; Williamson and Spencer, 1994). In the rat, high frequency stimulation in-vivo in the limbic status epilepticus model of epilepsy did reveal this type of phenomenon extracellularly as well (Sloviter, 1991b). Several possible explanations for the lack of multiple spikes in this study can be offered. These patients remained on their antiepileptic drug regimen up to the time of surgery. Furthermore, these patients were under light anesthesia with isoflurane and fentanyl during the recordings. Although all of these patients were refractory to medical therapy, these medications could conceivably affect stimulus induced epileptiform discharges.

One other observation of interest was the large late negativity seen in many of the patients. (See Figure 10) The neurotransmitter released by the perforant path terminals which seems to be involved in the generation of epileptiform activity is glutamate and both N-methyl-D-aspartate (NMDA) (Masukawa, et al., 1989; Urban, et al., 1990; Masukawa, et al., 1991; Williamson and Spencer, 1994) and non-NMDA receptors exist on the granule cells and can contribute to the observed waveforms (Lambert and Jones, 1989; Lambert and Jones, 1990). Urban et al. (1990) found a late negative component in 6 of 12 slices similar to the findings in this study and further showed that it was related to NMDA receptors. Several studies have indicated an association of NMDA related neuronal responses in the context of epilepsy (Masukawa, et al., 1989; Urban, et al., 1990; Masukawa, et al., 1991; Williamson and Spencer, 1994). Perhaps this is evidence of these types of changes in-vivo as well.

Loss of feedback inhibition

The results of the paired-pulse experiment revealed a loss of feedback inhibition at short IPIs as measured by the PS ratios in the dentate gyrus of patients with MTS compared to lesion patients. This was shown to be independent of EPSP changes through examination of the PS/EPSP and PS/EPSP slope ratios. Furthermore, this correlated with the degree of atrophy as measured by the hippocampal volume and with the number of years of seizures. This is in agreement with previous results in the limbic status epilepticus (Sloviter, 1991b; Sloviter, 1991a; Bekenstein, et al., 1993) and the kainate models (Sloviter and Damiano, 1981; Fisher and Alger, 1984; Cornish and Wheal, 1989; Sloviter, 1992) of epilepsy and in-vitro findings in resected tissue from humans with medial temporal lobe epilepsy (Isokawa, et al., 1991; Uruno, et al., 1994). This loss of feedback inhibition has been attributed to a loss of recurrent GABAergic input to the dentate granule cells (Andersen, et al., 1964; Matthews, et al., 1981; Alger and Nicoll, 1982; Thalman and Ayala, 1982; Tuff, et al., 1983; Peer and McLennan, 1986). Because of the preservation of GABA containing cells in human hippocampus resected for epilepsy (Babb, et al., 1989), it has been proposed that another cell type must be involved. One such cell that exists in the dentate hilus and has been shown to be lost in animal models is the mossy cell (Margerison and Corsellis, 1966; Mouritzen Dam, 1980; Babb, et al., 1984). Although no direct evidence of a loss mossy cells was sought in this study, the loss of these cells and their excitatory input to the inhibitory basket cells could possibly lead to such changes.

The results from some investigators utilizing the kindling model of epilepsy have revealed an increase in the amount of paired-pulse inhibition in the dentate gyrus (Tuff, et al., 1983; Oliver and Miller, 1985; de Jonge and Racine, 1987; Maru and Goddard, 1987; Stringer and Lothman, 1989; Robinson, 1991; Clusmann, et al., 1992; Zhao and Leung, 1992). This increase may be stimulus-intensity related; mild stimulation intensities revealed increased inhibition while higher stimulus intensities revealed a loss of this inhibition (Tuff,

et al., 1983; Stringer and Lothman, 1989; Kamphius, et al., 1992). Significantly, our stimulus intensity of 2 times threshold is not in excess of those used in the studies revealing increased inhibition. Overall, these results taken the finding a loss of inhibition suggest that the kindling model may not induce electrophysiological changes that are comparable to the human epileptic state, although differences in stimulation parameters cannot be ruled out. The one in-vivo human study (Isokawa-Akesson, et al., 1989) revealing increased inhibition was not performed with the knowledge of the location from which stimulation and recordings took place. This may explain the differences in their findings.

This loss of feedback inhibition did not correlate with neuronal loss or sprouting, while it was correlated with hippocampal volume loss. One possible explanation for this is that perhaps the hippocampal volume is a better measure of overall damage than the other measures. In addition, hippocampal volumetric measurements were available in 22 of the 23 patients while neuronal densities and immunohistochemistry for sprouting were only available for 20 and 18 patients respectively. It could be that with a greater N size, these measures would show a significant correlation.

The lack of significant changes in the EPSP or EPSP slopes between the two groups in the paired-pulse experiment is in agreement with the findings in several animal studies (de Jonge and Racine, 1987; Zhao and Leung, 1992). In addition, the mild facilitation of EPSP slopes that was observed at intermediate IPIs (See Figure 14) is consistent with the findings in these studies (Lomo, 1971b; Creager, et al., 1980; Joy and Albertson, 1987; Joy and Albertson, 1993). In a partial kindling model, Leung et al. (1994) found a mild depression in the EPSP slope ratios after kindling at IPIs from 20 to 200 msec. Although it did not reach significance, a similar trend was seen in the MTS patients compared to the lesion patients in this study (See Figure 14). One finding not previously reported in the literature is that of the mild inhibition of the population spike

observed in the MTS patients that did not seem to recover with time. This finding will be discussed further below on page 58.

Loss of feedforward inhibition and frequency related changes in the PS

Sloviter (1991a) reported an increase in inhibition of the first spike of a pair as stimulation frequency was increased from 0.1 to 1 Hz in normal rats and he attributed these findings to feedforward inhibition. This inhibition was subsequently lost as the stimulation frequency was further increased. In the limbic status epilepticus model of epilepsy, this feedforward inhibition has been shown to be lost compared to controls (Sloviter, 1991b). Our observations in the frequency experiment indicate that this type of feedforward inhibition is not present in either the MTS patients or the lesion patients.

Feedforward inhibition is felt to be mediated by a population of activity dependent neurons in the dentate hilus (Buzsaki, 1984; Sloviter, 1991a). The exact nature of the cells involved has not been well described, but conceivably, they may utilize the same circuitry for their final effects as proposed above - a connection to hilar mossy cells which in turn send excitatory input to the dentate basket cells.

Patients with lesion related epilepsy are thought to have their seizures arise outside the hippocampus with subsequent propagation to the hippocampus. This type of abnormal input could possibly cause excitotoxic damage to these feedforward interneurons as they receive direct afferent input via the perforant path. Because those neurons involved in feedback inhibition are not activated directly by the input, they may be relatively preserved. The fact that the granule cells remain relatively preserved in both medial temporal lobe epilepsy associated with lesions and MTS may reflect decreased susceptibility of these cells to excitotoxic damage. Our findings of intact feedback inhibition and diminished feedforward inhibition in the lesion patients is consistent with this.

This loss of feedforward inhibition was also seen in the MTS patients. Again, if the mossy cell - basket cell circuitry is the final effector of this type of inhibition, a loss of these mossy cells explains the finding of a loss of feedforward inhibition in the MTS patients as well.

In the normal rat (Andersen and Lomo, 1967; Tuff, et al., 1983; Sloviter, 1991a) population spike potentiation is reported in response to increasing stimulus frequency. Although the lesion patients did not demonstrate any marked potentiation, more striking was the finding that the MTS patients showed a progressive attenuation in the population spike at increased frequencies. The frequencies utilized in this experiment resulted in stimuli being administered every 333, 500, 1000, 5000 and 10000 msec for the 3, 2, 1, 0.2 and 0.1 Hz frequencies receptively. One possible explanation for our findings would be that the low-level inhibition observed in the paired-pulse experiments in the MTS patients at IPIs up to 200 msec still persisted to the time intervals listed above. Additionally, the findings of decreased PS/EPSP and PS/EPSP slope in MTS patients to single stimuli would also be consistent with this hypothesis of abnormal inhibition. One caveat to this theory is if the mechanism of generating the observed inhibition is dependent upon the discharge of the granule cells, the inhibition itself would also inhibit its own induction. This could lead to a response pattern where only every other (or more generally, every *n*th) stimulation results in granule cell discharge and thus the induction of this inhibition. Because an average of ten responses was utilized in summarizing this data, the inhibition could still possibly manifest itself in the final average.

A more attractive hypothesis could be offered as follows. Activity dependent facilitation in the hippocampus has been attributed to GABA binding to $GABA_B$ receptors on inhibitory cells (Mott, et al., 1993). The time range of the activity of this $GABA_B$ mediated disinhibition (200-400 ms) is almost identical to the corresponding interstimulus times for the frequencies at which we observed this loss of potentiation. If these activity dependent cells normally receive their input via mossy cells, the loss of this excitatory

input to these cells would result in a disinhibition of the inhibitory basket cells. Rather than observed potentiation, a progressive attenuation, as we have observed would result.

The lack of marked frequency related potentiation in the lesion patients may be abnormal as well. Some evidence comes from the finding that granule cells from patients with temporal lobe tumors display smaller afterhyperpolarizations compared to the normal rodent, have less spike frequency adaptation and less frequently display EPSP-IPSP sequences at subthreshold stimulating currents (Williamson, et al., 1993). These differences may indicate differences in the amount of feedforward inhibition and would be consistent with this hypothesis.

Frequency related changes in the EPSP height

Patients with significant cell loss in the dentate, CA4 or evidence of sprouting showed an *attenuation* of EPSP height with increasing stimulus frequency, while patients without these changes showed frequency related EPSP *potentiation*. Significant differences were only found for the EPSP amplitude ratios and not for the EPSP slope ratios. The literature in the past has almost exclusively utilized EPSP slopes as a measure of this presynaptic inhibition. Ahida et al. (1991) point out that it is the EPSP height that governs excitatory drive on an individual cell basis and that the EPSP slope is utilized only as a more convenient estimate of the EPSP height, because of difficulties in measuring this height when the EPSP is interrupted by the population spike. This would indicate that it is not unreasonable to use this measure in these correlations.

Few studies have provided detailed analysis of frequency related EPSP changes. White, et al. (1979) found at stimulus intensities subthreshold for the elicitation of population spikes, the extracellular EPSP showed a progressive attenuation as stimulation frequency was increased. Furthermore, these changes manifested themselves almost immediately after the initiation of stimulation at each frequency. This indicates that the method used in this study of two stimulations prior to the initiation of recording and

subsequent digitization and averaging of the following ten stimuli is adequate. Their observation would indicate that the observed potentiation associated with a lack of cell loss or reorganization in the dentate is abnormal. This seems paradoxical. Perhaps this frequency related potentiation is an early result of seizure damage and as cell loss and reorganization occurs, a restoration of this type of inhibition may occur. Evidence of a restoration of inhibition has been found in the kainate model, where sprouting was found to be associated with a restoration of feedback inhibition (Cronin, et al., 1992; Sloviter, 1992). Alternatively, the potentiation observed in those patients without these histological changes may be the result of increased presynaptic facilitation. This seems less likely because evidence of presynaptic mechanisms of facilitation in the hippocampus is lacking (Thompson, et al., 1993). Lastly, because these measures were performed at suprathreshold stimulus intensities rather than subthreshold, this fact alone may explain the differences observed.

Differences in PS/EPSP measures

For single low frequency stimuli, a significant difference in the ratio amplitude of the population spike to the EPSP amplitude and EPSP slope was observed between the MTS and lesion patients. In a more rigorous fashion, previous animal studies have looked at this phenomenon by generating full input/output (I/O) curves at a range of different stimulus intensities (King, et al., 1985; Maru and Goddard, 1987). This is done by plotting the population spike amplitude against the EPSP slope over the range of stimulus intensities studied. This was not performed in this study because of the time consuming nature of this type of experiment while the patient is under anesthesia. All of the stimulations in this study were performed at a stimulus intensity set to be twice the spike threshold (whenever a population spike was observed). These animal studies have shown a depression of the I/O curve after kindling. This finding is consistent with our findings of a decreased PS/EPSP and PS/EPSP.

A short mention should be made of the marked facilitation of the PS/EPSPslope ratio in the frequency experiment at 1 Hz for the lesion patients. Previous studies have indicated that synaptic efficacy may vary in a frequency dependent manner, but this was found at much higher frequencies (4-8 Hz) and over a much broader range (Greenstein, et al., 1988; Munoz, et al., 1991). Our findings may result from a similar phenomenon, but it is unusual that such a narrow band exists. Furthermore, these measurements were only performed on three of the patients in the lesion group, although a relatively small variance is seen among them. Whether this finding is simply a statistical anomaly or truly represents a significant finding will await further study.

Verification of placement

The difficulties is locating the electrolytic lesions after stimulation led to the verification of electrode placement in only six patients. Some of the difficulties arose from the fact that often times vibratome sectioning of the hard sclerotic hippocampi resulted in minuscule tears which were difficult to separate from the actual lesion. The consistency between the observed waveforms with the lesion location in those patients in which lesions were identified and the consistent use of exactly the same methods for placement lead us to believe that in those patients where no lesion was located, the recording site was also in the dentate gyrus. Other studies have revealed that although the particular type of electrodes used provide a relatively poor spatial resolution, recordings from the dentate hilus have a small spatial rate of change of potential following perforant path stimulation (McNaughton, 1980). The other area which may be questioned as giving rise to the observed potentials is CA1, since the elctrode passes through this area on the way to the dentate granule cell layer. We believe that it is unlikely that CA1 was responsible for the observed waveforms for the following reasons. First, stimulation was begun at subthreshold levels and then increased until a population spike was observed. If CA1 was being excited both through direct perforant path afferents and via a multisynaptic pathway

through the dentate, one would expect to observe evidence of two responses with different latencies, as the stimulation current was increased. This was never observed. Second, in the MTS patients CA1 is an unlikely source of observable field potentials because of the typical severe cell loss in CA1 seen in MTS patients. Lastly, the depth at which the waveforms were observed was in all cases at least 3 mm from the surface, well beyond the depth at which the CA1 pyramidal cell layer exists.

The existence of direct entorhinal afferent connections to CA1 has been demonstrated both anatomically and electrophysiologically (Doller and Weight, 1982; Colbert and Levy, 1992), but their significance with regard to evoked field responses has been questioned. Yeckel and Berger (1990) showed that the short latency monosynaptic response recorded in CA1 when the dentate is also activated consists primarily of a large positivity which is volume conducted from the dentate. Only after selective inhibition of the dentate population spike was a small response, uncontaminated by the previously observed large positivity uncovered. When monosynaptic discharges were observed, they were commonly followed by EPSP's of latencies corresponding to disynaptic and trisynaptic input. Further careful study by Stringer and Colbert (1994) revealed that when the dentate discharge was inhibited by a preceding shock to the contralateral hilus (this is known to cause inhibition in the dentate via commisural mossy cell projections in animals), the response in the dentate gyrus and CA1 was decreased equally. Current source density analysis further confirmed that this early response was volume conducted by revealing that early current sinks were located only in the dentate gyrus. The above evidence makes the likelihood that the recorded responses originated in CA1 extremely small.

Limitations of the study

This study was carried out in a limited number of patients which represent a heterogeneous cross section of patients with medically refractory temporal lobe epilepsy who qualified as surgical candidates. The findings of this study, therefore, may not apply

to all patients with temporal lobe epilepsy. Furthermore, there was substantial variation in the number and type of seizures experienced, as well as the type of mass lesions. A more uniform group might have had greater statistical power in finding correlations between variables.

A concern in many of the studies utilizing brain from epileptic subjects is the unknown effect of long-term antiepileptic drug use on the electrophysiological properties of the tissue (Williamson, et al., 1993). Furthermore, in this study, the patients remained on their anti-epileptic drugs up to the morning of their surgery. A study of these patients while not under the influence of antiepileptic medication might have revealed greater evidence of hyperexcitablity and loss of inhibition, but the fact remains that these patients were selected as surgical candidates because they continued to experience seizures despite maximal medical therapy, thus giving evidence that an abnormal state of excitability remains even in the face of medication.

Summary

Synthesis of a model of inhibition in the hippocampus

Overall, this study found evidence of both a loss of inhibition and a gain in seemingly abnormal inhibition. The paired pulse study revealed a relative loss of feedback inhibition in the MTS patients compared to the lesion patients at short interpulse intervals consistent with a loss of excitatory input to the GABAergic feedback inhibitory circuits in the dentate gyrus. Further, the MTS patients seemed to have a low-level of dysfunctional feedback inhibition which was slow to recover with time. Neither set of patients manifested feedforward inhibition, but the MTS patients showed an abnormal progressive attenuation of the population spike as frequency of stimulation increased. This is consistent with a loss of GABAergic input to activity dependent inhibitory circuits which

was manifested as a loss of potentiation. Evidence that sprouting along with dentate granule cell loss and CA4 cell loss may restore elements of EPSP frequency related inhibition was also found.

A model explaining the results has been alluded to in the above discussion and is presented in summary in Figure 35 on pages 67-68. The paired pulse inhibition normally provided by mossy cell input is lost in patients with MTS. As frequency is increased, granule cell output is initially suppressed by direct perforant path input to activity dependent excitatory cells. These cells are proposed to be lost due to excitotoxic insult in the lesion patients, while their target, the mossy cells are lost in the MTS patients. As frequency is further increased, the feedforward circuit is unable to fully suppress the granule cells. The granule cell output then activates activity dependent inhibitory cells via recurrent synapses to mossy cells. Inhibition by basket cells is then attenuated allowing potentiation to occur. This attenuation is lost in the MTS patients due to the loss of the mossy cells. This attenuation would require excitatory input in order for this to take place. Although two basket cells are shown for simplicity in the figure, it may be that the same basket cell that is receiving inhibitory input from activity dependent cells also receives excitatory feeforward and feedback input. With the loss of inhibitory input, this basket cell would then become active, causing the observed attenuation.

In the creation of a model, it is necessary to be somewhat reductionistic for simplicity. Certainly, many more influences on these cells may be present than illustrated in the figures. Most likely, all of these circuits are active all of the time, but the balance between them is altered both in the paradigms used in this experiement and in the different disease states. Central in this model are the proposal of a loss of mossy cells in patients with MTS and the presence of activity dependent interneurons. A further discussion of these cells in given below.

Mossy Cells

Mossy cells are the most common type of cell in the dentate hilus of the rat (Amaral, 1978).. They receive input from a number of sources including the perforant path and via mossy fiber collaterals from the dentate granule cells. (This nomenclature is confusing: mossy *cells* receive input from granule cells via mossy *fibers*.) Overwhelming evidence exists that mossy cells are excitatory (Storm-Mathison, et al., 1983; Ribak, et al., 1985; Buckmaster, et al., 1992; Soriano and Frotscher, 1994). Their main axonal projections extend to the ipsilateral and contralateral inner molecular layer of the dentate gyrus, (Berger, et al., 1980; Ribak, et al., 1985; Buckmaster, et al., 1992) where interneurons and their processes such as the basket cells are located. It has been documented that these cells are lost in human medial temporal lobe epilepsy (Margerison and Corsellis, 1966; Mouritzen Dam, 1980; Babb, et al., 1984) and in the limbic status epilepticus model, (Sloviter, 1987; Scharfman, et al., 1990) but, unfortunately, no direct immunohistochemical methods are available to conveniently study this loss (Ribak, et al., 1985). The loss of these cells could possibly explain all of the findings of changes in the population spikes in patients with MTS in the study because of their proposed pivotal role in providing excitatory input to the dentate basket cells and the activity dependent inhibitory cells. Perhaps more detailed histological study, such as those used in the studies quoted above (Margerison and Corsellis, 1966; Mouritzen Dam, 1980; Babb, et al., 1984; Sloviter, 1987; Scharfman, et al., 1990), might have revealed such losses.

Activity dependent interneurons

In the model, we propose that two separate sets of activity dependent interneurons exist; one excitatory, the other inhibitory. Several studies have indicated that components of inhibition in the hippocampus are activity dependent (Ben Ari, et al., 1979; McCarren and Alger, 1985; Thompson and Gahwiler, 1989; Davies, et al., 1990; Otis and Mody, 1992). The existence of these activity dependent excitatory neurons has been proposed by Sloviter (Sloviter, 1991b) as being partially responsible for feedforward inhibition at

medium frequencies of stimulation (1 Hz), although no direct evidence for the existence of these cells was given. Mott et al. (1993) found strong evidence that the activity dependent depression of mossy fiber evoked polysynaptic inhibition is mediated by $GABA_B$ receptors on inhibitory cells. $GABA_B$ receptors have been found on inhibitory neurons on somites, dendrites and near the axon terminals where they may either produce a late IPSP or directly inhibit GABA release (Harrison, 1990; Scharfman, et al., 1990; Lacaille, 1991; Lambert, et al., 1991). Again, the precise cells mediating this function have not been identified, but it seems that substantial evidence exists to postulate their role in the inhibitory processes studied. It may be that this activity dependent function is not manifested by any particular cell, but is a population phenomenon which is the net result of combinations of potentiation and inhibition of differing intensities and time durations that combine to allow a greater number of cells to discharge in a frequency dependent manner.

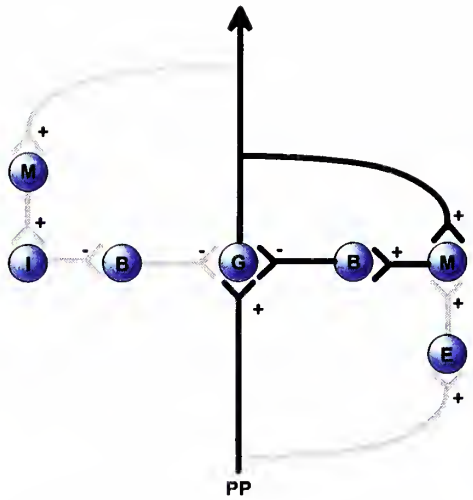

Normal - Low Frequency Paired Pulse

At low frequencies, in the normal dentate gyrus, feed back inhibition predominates through recurrent collaterals to mossy cells which in turn give excitatory input to inhibitory basket cells

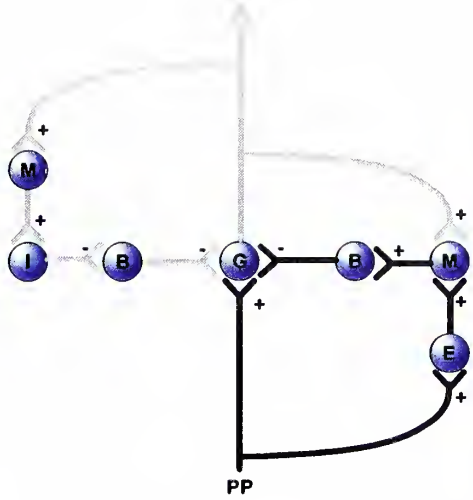

Normal - Medium Frequency Single Stimuli

At medium frequencies, the feedforward circuit of perforant path to activity dependent excitatory cells which in turn synapse on mossy cells predominates. The mossy cells then excite the inhibitory basket cells.

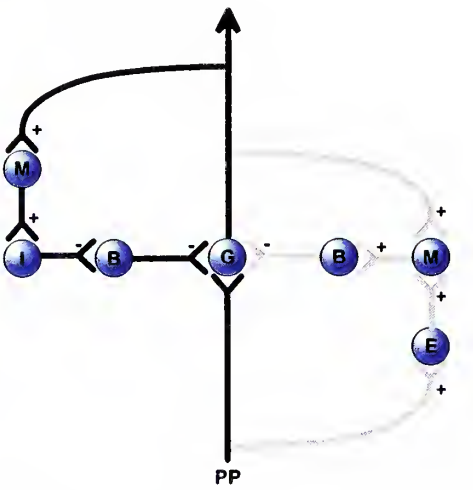

Normal - High Frequency Single Stimuli

At high frequencies, potentiation of the population spike occurs via input to mossy cells which then synapse on activity dependent inhibitory cells. These cells then diminish the basket cells inhibitory response. Although this is shown as a recurrent input, direct input to the mossy cells may also come from the perforant path.

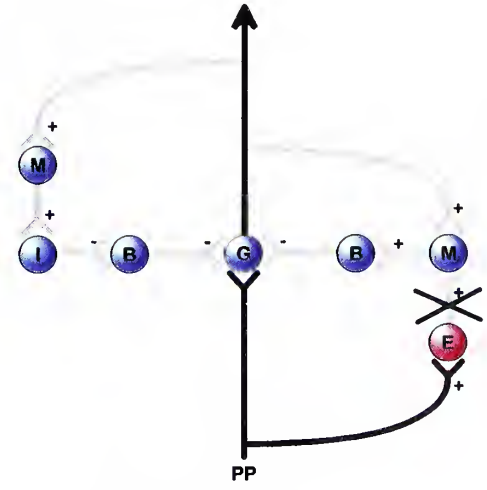

Lesion - Medium Frequency Single Stimuli

In the lesion paticnts, excitotoxic damage occurs to the activity dependent excitatory cells, causing a loss of feedforward inhibition.

Figure 35: Model of dentate inhibitory circuits. The pathways shown in black represent the dominant pathway. "X"s represent cells that are lost. Legend: **PP** Perforant path fibers; **G** Granule cell; **B** Basket cell; **M** Mossy cell; **E** Activity dependent excitatory cell; **I** Activity dependent inhibitory cell.

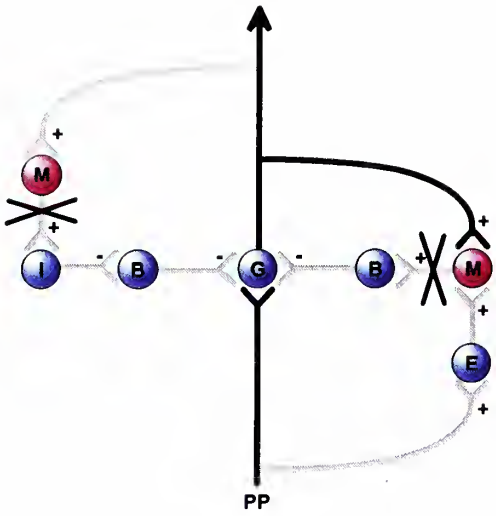

MTS - Low Frequency Paired Pulse

At low frequencies, in the MTS patients, feedback inhibition is lost due to the loss of hilar mossy cells and their excitatory input to inhibitory basket cells.

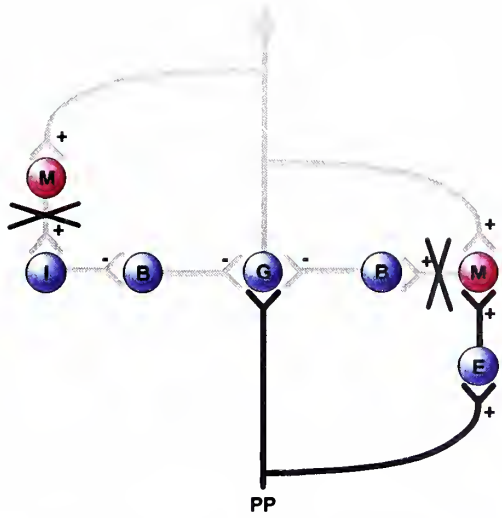

MTS - Medium Frequency Single Stimuli

At medium frequencies, feedforward inhibition is lost as well due to the loss of mossy cells.

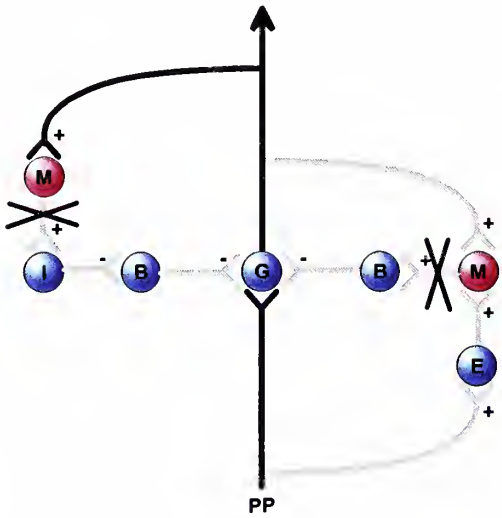

MTS - High Frequency Single Stimuli

At high frequencies, the potentiation which exists in the normal situation is lost through the loss of mossy cells and their excitatory input to the activity dependent inhibitory cells.

Figure 35 (cont.): Model of dentate inhibitory circuits. The pathways shown in black represent the dominant pathway. "X"s represent lost cells. Legend: **PP** Perforant path fibers; **G** Granule cell; **B** Basket cell; **M** Mossy cell; **E** Activity dependent excitatory cell; **I** Activity dependent inhibitory cell.

Conclusion

The major findings of this study are 1) the loss of feedback inhibition in the hippocampi of MTS patients compared to tumor patients, 2) the loss of early feedback inhibition in both sets of patients and 3) a loss of frequency related potentiation in patients with MTS. The findings in this study of a loss of feedback and feedforward inhibition confirm the findings in selected previous animal and in-vitro human studies as detailed above. In addition, several new findings of 1) the loss of frequency related potentiation in the MTS patients, 2) correlations of the loss of inhibition with hippocampal volumes and the duration of seizures and 3) the correlations of changes in the EPSP ratio with histological variables may shed new light on the state of the inhibitory circuits in the hippocampus of patients with temporal lobe epilepsy. These changes in inhibition indicate possible mechanisms by which the hippocampus becomes a source for the generation of seizures or becomes the area to which epileptic discharges spread most commonly. The precise events that occur in order to initiate a seizure remain elusive, but the observations of changes in inhibition at different frequencies may indicate a preferential spread of certain types of discharges. Alternatively, because these studies were performed with stimulation of the perforant path, the loss of potentiation at higher frequencies in the MTS patients may indicate that this pathway may not be significantly involved in the initiation of seizures to or from the hippocampus; future study of the intrinsic pathways may provide further clues to the mechanisms by which the hippocampus becomes a source of ictal events. The results of this study may lead to new strategies of diagnostic and therapeutic interventions. The fact that this information is available prior to resection may possibly aid in the decisions regarding the resection of the hippocampus at surgery. Furthermore, the development of a model by which these changes in inhibition occur provides a substrate for further directed study and indicates possible avenues by which new pharmacological interventions may take place.

REFERENCES

Abercrombie, M. (1946). Estimation of the nuclear population from microtome section. **Anat Rec** 94:239-247.

Ahida, H., Maru, E., and Tatsung, J. (1991). Time discrete model of recurrent inhibition in hippocampal dentate gyrus. **J Theor Biol** 148:1-16.

Albertson, T. E., Tseng, C. C., and Joy, R. M. (1991). Propofol modification of evoked hippocampal dentate inhibition in urethane-anesthetized rats. **Anesthesiology** 75:82-90.

Albertson, T. E., Walby, W. F., and Joy, R. M. (1992). Modification of GABA-mediated inhibition by various injectable anesthetics. **Anesthesiology** 77:488-99.

Alger, B. E., and Nicoll, R. A. (1982). Feed-forward dendritic inhibition in rat hippocampal pyramidal cells studied in vitro. **J Physiol** 328:105-23.

Amaral, D. G. (1978). A Golgi study of cell types in the hilar region of the hippocampus in the rat. **J Comp Neurol** 182:851-914.

Amaral, D. G., and Insausti, R. (1990). The hippocampal formation. In G. Paxinos (Eds.), **The Human Nervous System** (pp. 711-55). New York: Academic Press.

Andersen, P., Bliss, T. V. P., and Skrede, K. K. (1971). Lamellar organization of hippocampal excitatory pathways. **Experimental Brain Research** 13:222-238.

Andersen, P., Eccles, J. C., and Loyning, Y. (1964). Pathway of postsynaptic inhibition in the hippocampus. **J Neurophysiol** 27:608-19.

Andersen, P., Holmqvist, B., and Voorhoeve, P. E. (1966a). Entorhinal activation of dentate granule cells. **Acta Physiologica Scandinavia** 66:448-460.

Andersen, P., Holmqvist, B., and Voorhoeve, P. E. (1966b). Excitatory synapses on hippocampal apical dendrites activated by entorhinal stimulation. **Acta Physiol Scand** 66:461-72.

Andersen, P., and Lomo, T. (1967). Control of hippocampal output by afferent volley frequency. **Prog Brain Res** 27:400-12.

Babb, T. L., and Brown, W. J. (1987). Pathological findings in epilepsy. In J. J. Engel (Eds.), **Surgical Treatment of the Epilepsies** (pp. 511-40). New York: Raven Press.

Babb, T. L., Kupfer, W. R., Pretorious, J. K., et al. (1991). Synaptic reorganization by mossy fibers in human epileptic fascia dentata. **Neuroscience** 42:351-363.

Babb, T. L., Lieb, J. P., Pretorius, J., and Crandall, P. H. (1984). Distribution of pyramidal cell density and hyperexcitability in the epileptic human hippocampal formation. **Epilepsia** 25:721-8.

Babb, T. L., Pretorious, J. K., Kupfer, W. R., and Crandall, P. H. (1989). Glutamate decarboxylase immunoreactive neurons are preserved in human epileptic hippocampus. **Journal of Neuroscience** 9:2562-2578.

Barnes, C. A. (1979). Memory deficits associated with senescence: a neurophysiological and behavioral study in the rat. **J Comp Physiol Psychol** 93:74-104.

Beckstead, R. M. (1978). Afferent connections to the entorhinal area in the rat as studied retrograde cell labeling with horseradish peroxidase. **Brain Res** 152:249-64.

Bekenstein, J., Rempe, D., and Lothamn, E. (1993). Decreased heterosynaptic and homosynaptic paired pulse inhibition as a chronic sequela to limbic status epilepticus. **Brain Res** 601:111-20.

Bekenstein, J. W., and Lothman, E. W. (1993). Dormancy of inhibitory interneurons in a model of temporal lobe epilepsy. **Science** 259:97-100.

Ben Ari, Y. (1985). Limbic seizure and brain damage produced by kainic acid: mechanisms and relevance to human temporal lobe epilepsy. **Neuroscience** 14:375-403.

Ben Ari, Y., Krnjevic, K., and Reinhardt, W. (1979). Hippocampal seizures and failure of inhibition. **Can J Physiol Pharmacol** 57:1462-6.

Berger, T. W., Semple-Rowland, S., and Basset, J. L. (1980). Hippocampal polymorph neurons are the cells of origin for ipsilateral and commisural afferents to the dentate gyrus. **Brain Res** 215:329-36.

Bertram, E. H., Lothman, E. W., and Lenn, N. J. (1990). The hippocampus in experimental chronic epilepsy: a morphometric analysis. **Ann Neurol** 27:43-8.

Blackstad, T. W. (1958). On the termination of some afferents to the hippocampus and fascia dentata. **Acta Anat** 35:202-14.

Bowery, N. G. (1989). GABA-B receptors and their significance in mammalian pharmacology. **Trend Pharmacol Sci** 10:401-7.

Brucato, F. H., Morrisett, R. A., Wilson, W. A., and Swartzwelder, H. S. (1992). The $GABA_B$ receptor antagonist, CGP-35348, inhibits paired-pulse disinhibition in the rat dentate gyrus in vivo. **Brain Res** 588:150-3.

Bruton, C. J. (1988). **The Neuropathology of Temporal Lobe Epilepsy**. London: Oxford University Press.

Buckmaster, P. S., Strowbridge, B. W., Kunkel, D. D., et al. (1992). Mossy cell axonal projections to the dentate gyrus molecular layer in the rat hippocampal slice. **Hippocamus** 2:349-62.

Buzsaki, G. (1984). Feed-forward inhibition in the hippocampal formation. **Prog Neurobio** 22:131-153.

Buzsaki, G., and Eidelberg, E. (1982). Direct afferent excitation and long-term potentiation of hippocampal interneurons. **J Neurophysiol** 48:597-607.

Cavalheiro, E. A., Riche, D. A., and Le Gal La Salle, G. (1982). Long-term effects of intrahippocampal kainic acid injection in rats: a method for inducing spontaneouas recurrent seizures. **EEG Clin Neurophysiol** 53:581-9.

Cavanagh, J. B., and Meyer, A. (1956). Aetotiological aspects of Ammon's horn sclerosis associated with temporal lobe epilepsy. **British Medical Journal** 2:1403-1407.

Clusmann, H., Stabel, J., Stephens, D. N., and Heinemann, U. (1992). Alterations in medial perforant path and mossy fiber induced field potentials in amygdala and beta-carboline (FG 7142) kindled rats. **Neurosci Lett** 146:65-8.

Colbert, C. M., and Levy, W. B. (1992). Electrophysiological and pharmacological characterization of perforant path synapses in CA1: mediation by glutamate receptors. **J Neurophysiol** 68:1-8.

Cornish, S. M., and Wheal, H. V. (1989). Long-term loss of paired pulse inhibition in the kainic acid-lesioned hippocampus of the rat. **Neuroscience** 28:563-71.

Creager, R., Dunwiddle, T., and Lynch, G. (1980). Paired-pulse and frequency facilitation in the CA1 region of the in-vitro rat hippocampus. **J Physiol** 299:409-24.

Cronin, J., and Dudek, F. E. (1988). Chronic seizures and collateral sprouting of dentate mossy fibers after kainic acid treatment in rats. **Brain Res** 474:181-4.

Cronin, J., Obenaus, A., Houser, C. R., and Dudek, F. E. (1992). Electrophysiology of dentate granule cells after kainate-induced synaptic reorganization of the mossy fibers. **Brain Res** 573:305-10.

Currie, S., Heatherfield, K. W. G., Henson, R. A., and Scott, D. F. (1971). Clinical course and prognosis of temporal lobe epilepsy. A survey of 666 patients. **Brain** 94:173-190.

Davenport, C. J., Brown, W. J., and Babb, T. L. (1990). Sprouting of GABAergic and mossy fiber axons in dentate gyrus following intrahippocampal kainate in the rat. **Exp Neurol** 109:180-90.

Davies, C. H., Davies, S. N., and Collinridge, G. L. (1990). Paired-pulse depression of monosynaptic GABA-mediated inhibitory postsynaptic responses in rat hippocampus. **J Physiol** 424:513-31.

de Jonge, M., and Racine, R. J. (1987). The development and decay of kindling-induced increases in paired-pulse depression in the dentate gyrus. **Brain Res** 412:318-28.

de Lanerolle, N. C., Brines, M. L., Kim, J. H., et al. (1992). Neurochemical remodelling of the hippocampus in human temporal lobe epilepsy. **Epilepsy Res Suppl** 9:205-19.

de Lanerolle, N. C., Kim, J. H., Robbins, R. J., and Spencer, D. D. (1989). Hippocampal interneuron loss and plasticity in human temporal lobe epilepsy. **Brain Res** 495:387-95.

Doller, H. J., and Weight, F. F. (1982). Perforant pathway activation of hippocampal CA1 stratum pyramidale neurons: electrophysiological evidence for a direct pathway. **Brain Res** 237:1-13.

Dudek, F. E., Obenaus, A., Schweitzer, J. S., and Wuarin, J. P. (1994). Functional significance of hippocampal plasticity in epileptic brain: electrophysiological changes of the dentate granule cells associated with mossy fiber sprouting. **Hippocampus** 4:259-265.

During, M. J., and Spencer, D. D. (1993). Extracellular hippocampal glutamate and spontaneous seizure in the conscious human brain **Lancet** 341:1607-10.

Dutar, P., and Nicoll, R. A. (1988a). A physiological role for GABA-B receptors in the cenral nervous sytem. **Nature** 332:156-8.

Dutar, P., and Nicoll, R. A. (1988b). Pre- and postsynaptic GABA-B receptors in the hippocampus have different pharmacological properties. **Neuron** 1:585-91.

Duvernoy, H. M. (1988). **The Human Hippocampus**. Munchen: J. F. Bergmann Verlag.

Engel, J. J. (1981). Correlation o fcriteria using for localizing epileptic foci in patients in patients considered for surgical therapy in epilepsy. **Ann Neurol** 9:215-24.

Engel, J. J., Driver, M. V., and Falconer, M. A. (1975). Electrophysiological correlates of pathology and surgical results in temporal lobe epilepsy. **Brain** 98:129-56.

Feldblum, S., and Ackermann, R. (1987). Increased susceptibility to hippocampal and amygdala knidling following intrahippocampal kainic acid. **Exp Neurol** 97:225-69.

Fisher, R. S., and Alger, B. E. (1984). Electrophysiological mechanisms of kainic acid-induced epileptiform activity in the rat hippocampal slice. **J Neurosci** 4:1312-23.

Franck, J., and Schwartzkroin, P. (1985). Do kainaite-lesioned hippocampi become epileptogenic? **Brain Res** 329:309-13.

Fried, I., Kim, J. H., and Spencer, D. D. (1992). Hippocampal pathology in patients with intractable seizures and temporal lobe masses. **J Neurosurg** 76:735-40.

Gastaut, H. (1953). So-called "psychomotor" and "temporal" epilepsy. **Epilepsia** 5:59-99.

Gastaut, H., and Gastaut, J. L. (1976). Computerized transverse axial tomography in epilepsy. **Epilepsia** 17:325-336.

Gastaut, H., Gastaut, J. L., Goncalves e Silva, G. E., and Fernandez Sanchez, G. R. (1975). Relative frequency of different types of epilepsy: a study employing the classification of epileptic seizures. **Epilepsia** 16:457-61.

Goddard, G. V., McIntyre, D. C., and Leech, C. K. (1969). A permanent change in brain function resulting from daily electrical stimulation. **Exp Neurol** 25:295-330.

Greenstein, Y., Pavlides, C., and Winson, J. (1988). Long-term potentiation in the dentate gyrus is preferentially induced at theta rhythm periodicity. **Brain Res** 438:331-334.

Haglund, M. M., Berger, M. S., Kunkel, D. D., and al, e. (1992). Changes in gamma-aminobutyric acid and somatostatin in epileptic cortex associated with low-grade gliomas. **J Neurosurg** 77:209-216.

Harris, E. W., Lasher, S., and Steward, O. V. (1979). Analysis of habituation-like changes in transmission in temporo-dentate pathway of the rat. **Brain Res** 162:219-32.

Harrison, N. L. (1990). On the presynaptic action of baclofen at inhibitory synapses between cultured rat hippocampal neurones. **J Physiol** 422:433-46.

Hauser, W. A., and Kurkland, L. T. (1975). The epidemiology of epilepsy in Rochester, Minnesota, 1935-1967. **Epilepsia** 16:1-66.

Henry, T. R., Chugani, H. T., Abou-Khalil, B. W., and Theodore, W. H. (1993). Postitron emmision tomography. In J. J. Engel (Eds.), **Surgical Treatment of the Epilepsies** (pp. 211-32). New York: Raven Press.

Hjorth-Simonsen, A. (1973). Projection of the lateral part of the entorhinal area to the hippocampus and fascia dentata. **J Comp Neurol** 1972:219-232.

Hjorth-Simonsen, A., and Jeune, B. (1972). Origin and termination of the perforant path in the rat studied by silver impregnation. **J Comp Neurol** 144:215-232.

Houser, C. R. (1990). Granule cell dispersion in the dentate gyrus of humans with temporal lobe epilepsy. **Brain Res** 535:195-204.

Houser, C. R., Miyashiro, J. E., Swartz, B. E., et al. (1990). Altered patterns of dynorphin immunoreactivity suggest mossy fiber reorganization in human hippocampal epilepsy. **J Neurosci** 10:267-82.

Isokawa, M., Avanzini, G., Finch, D. M., et al. (1991). Physiologic properties of human dentate granule cells in slices prepared from epileptic patients. **Epilepsy Res** 9:242-50.

Isokawa, M., Levesque, M. F., Babb, T. L., and Engel, J., Jr. (1993). Single mossy fiber axonal systems of human dentate granule cells studied in hippocampal slices from patients with temporal lobe epilepsy. **J Neurosci** 13:1511-22.

Isokawa-Akesson, M., Wilson, C. L., and Babb, T. L. (1989). Inhibition in synchronously firing human hippocampal neurons. **Epilepsy Research** 3:236-247.

Joy, R. M., and Albertson, T. E. (1987). Interactions of lindane with synaptically mediated inhibition and facilitation in the dentate gyrus. **Neurotoxicology** 8:529-42.

Joy, R. M., and Albertson, T. E. (1993). NMDA receptors have a dominant role in population spike-paired pulse facilitation in the dentate gyrus of urethane-anesthetized rats. **Brain Res** 604:273-82.

Kamphius, W., Gorter, J. A., Wadman, W. J., and Lopes da Silva, F. H. (1992). Hippocampal kindling leads to different changes in paired-pulse depression of local evoked field potentials in CA1 area and in fascia dentata. .

Kamphius, W., Wadman, W. J., and Lopes da Silva, F. H. (1988). Changes in local evoked potentials in the rat hippocampus (CA1) during kindling epileptogenesis. **Brain Res** 440:205-215.

Kamphuis, W., Wadman, W. J., Buits, R. M., and Lopes da Silva, F. H. (1986). Decrease in number of hippocampal gamma-aminobutyric acid (GABA) immunoreactive cells in the rat kindling model. .

Kandel, E. R., Spencer, W. A., and Brinkley, F. J. (1961). Electrophysiology of hippocampal neurons. I. Sequential invasion and synaptic organization. **J Neurophys** 24:225-42.

Kapur, J., Bennett, J., Jr., Wooten, G. F., and Lothman, E. W. (1989). Evidence for a chronic loss of inhibition in the hippocampus after kindling: biochemical studies. **Epilepsy Res** 4:100-8.

Kapur, J., and Lothamn, E. W. (1989). Loss of recurrent inhibition precedes delayed spontaneous seizures in the hippocampus after tetanic electrical stimulation. **J Neurophsiol** 61:426-34.

Kapur, J., Michelson, H. B., Buterbaugh, G. G., and Lothman, E. W. (1989). Evidence for a chronic loss of inhibition in the hippocampus after kindling: electrophysiological studies. **Epilepsy Res** 4:90-9.

Keppel, G. (1973). **Design and Analysis: A Researcher's Handbook**. Englewood Cliffs: Prentice Hall.

Kim, J. H., Guimaraes, P. O., Shen, M. Y., et al. (1990). Hippocampal neuronal density in temporal lobe epilepsy with and without gliomas. **Acta Neuropathol** 80:41-5.

Kim, J. H., Kraemer, D. L., and Spencer, D. D. (1995). The neuropathology of epilepsy. In A. Hopkins, S. Shorvon, and G. Cascino (Eds.), **Epilepsy**

King, G. L., Dingledine, R., Giacchino, J. L., and McNamara, J. O. (1985). Abnormal neuronal excitability in hippocampal slices from kindled rats. **J Neurophysiol** 54:1295-1304.

Knowles, W. D., Awad, I. A., and Nayel, M. H. (1992). Differences of in vitro electrophysiology of hippocampal neurons from epileptic patients with mesiotemporal sclerosis versus structural lesions. **Epilepsia** 33:601-609.

Krettek, J. E., and Prince, J. L. (1977). Projections from the amygdaloid complex and adjacent olfactory structures to the entorhinal cortex and to the subiculum in the rat and the cat. **J Comp Neurol** 172:723-52.

Krnjevic, K. (1974). Chemical nature of synaptic transmission in vertebrates. **Physiol Rev** 54:418-540.

Krug, M., Bergado, J., and Ruethrich, H. (1990). Long-term potentiation and postconditioning potentiation - the same mechanism? **Biomed Biochem Acta** 49:273-9.

Kuzniecky, R., De la Sayette, V., Ethier, R., et al. (1987). Magnetic resonance imaging in temporal lobe epilepsy: pathological correlations. **Annals of Neurology** 22:341-347.

Lacaille, J.-C. (1991). Postsynaptic potentials mediated by excitatatory and inhibitory amino acids in interneurons of stratum pyramidale of the CA1 region in area CA1 of rat hippocampal slices in-vitro. **J Neurophysiol** 66:1141-54.

Lambert, J. D. C., and Jones, R. S. G. (1989). Activation of N-methyl-D-aspartate receptors contributes to the EPSP at perforant path synapses in the rat dentate gyrus in vitro. **Neurosci Lett** 97:323-8.

Lambert, J. D. C., and Jones, R. S. G. (1990). A reevaluation of excitatory amino acid-mediated synaptic transmission in rat dentate gyrus. **J Neurophysiol** 64:119-32.

Lambert, N. A., Harrison, N. L., and Teyler, T. J. (1991). Baclofen-induced disinhibition in area CA1 of rat hippocampus is resistant to to extracellulat Ba2+. **Brain Res** 547:349-52.

Lancaster, B., and Wheal, H. V. (1982). A comparative histological and electrophysiological study of some neurotoxins in the rat hippocampus. **J Comp Neurol** 211:105-114.

Laurberg, S., and Sorensen, K. E. (1981). Associational and commisural collaterals of neurons in the hippocampal formation (hilus fasciae dentatae and subfield CA3). **Brain Res** 212:287-300.

Laurberg, S., and Zimmer, J. (1981). Lesion-induced sprouting of hippocampal mossy fiber collaterals to the fascia dentata in developing and adult rats. **J Comp Neurol** 200:433-59.

Leibowitz, N. R., Pedley, R. A., and Cutler, R. W. P. (1978). Release of gamma-aminobutyric acid from hippocampal slices of the rat following generalized sizures induced by daily electrical stimulation of entorhinal cortex. **Brain Res** 138:369-73.

Lencz, T., McCarthy, G., Bronen, R. A., et al. (1992). Quantitative magnetic resonance imaging in temporal lobe epilepsy: relationship to neuropathology and neuropsychological function. **Ann Neurol** 31:629-37.

Leung, L. S., Zhao, D., and Shen, B. (1994). Long-lasting effects of partial hippocampal kindling on hipocampal physiology and function. **Hippocampus** 4:696-704.

Lomo, T. (1968). Nature and distribution of inhibition in a simple cortex (dentate area). **Acta Physiol Scand** 74:8A-9A.

Lomo, T. (1971a). Patterns of activation in a monosynaptic cortical pathway: The perforant path input to the dentate area of the hippocampal formation. **Experimental Brain Research** 12:18-45.

Lomo, T. (1971b). Potentiation of monosynaptic EPSPs in the perforant path-dentate granule cell synapse. **Exp Brain Res** 12:46-63.

Lorente de No, R. (1934). Studies on the structure of the ccerebral cortex. II. Continuation of the study of the ammonic system. **J Psychol Neurol** 46:113-177.

Lothman, E. W., Bertram, E. H., Kapur, J., and Stringer, J. L. (1990). Recurrent spontaneous hippocampal seizures in the rat as a chronic sequela to limbic status epilepticus. **Epilepsy Res** 6:110-8.

Magerison, J. H., and Corsellis, J. A. N. (1966). Epilepsy and the temporal lobes, a clinical, electrographic and neuropathological study of the brain in epilepsy, with particular reference to the temporal lobes. **Brian** 89:499-530.

Margerison, J. H., and Corsellis, J. A., N. (1966). Epilepsy and the temporal lobes. **Brain** 89:499-529.

Maru, E., Ashida, H., and Tatsuno, J. (1989). Long-lasting reduction of paired-pulse depression following LTP-inducing tetanic stimulations of the perforant path. **Brain Res** 478:112-20.

Maru, E., and Goddard, G. V. (1987). Alterations in dentate activities associated with perforant path kindling III. Enhancement of synaptic inhibition. **Exp Neurol** 96:46-60.

Masukawa, L. M., Higashima, M., Hart, G. J., et al. (1991). NMDA receptor activation during epileptiform responses in the dentate gyrus of epileptic patients. **Brain Res** 562:176-80.

Masukawa, L. M., Higashima, M., Kim, J. H., and Spencer, D. D. (1989). Epileptiform discharges evoked in hippocampal brain slices from epileptic patients. **Brain Res** 493:168-74.

Masukawa, L. M., Uruno, K., Sperling, M., et al. (1992). The functional relationship between antidromically evoked field responses of the dentate gyrus and mossy fiber reorganization in temporal lobe epileptic patients. **Brain Res** 579:119-27.

Matthews, W. O., McCafferty, G. P., and Setler, P. E. (1981). An electrophysiological model of GABA-mediated neurotransmission. **Neuropharmacology** 20:561-5.

McCarthy, G., and Luby, M. (1994) Imaging the structural changes with human epilepsy.**Clin Neuroscience** 2:82-8.

McCarren, M., and Alger, B. E. (1985). Use dependent depression of IPSP's in hippocampal cells in vitro. **J Neurophysiol** 53:557-71.

McDonald, J. W., Garofalo, E. A., Hood, T., et al. (1991). Altered excitatory and inhibitory amino acid receptor binding in hippocampus of patients with temporal lobe epilepsy. **Ann Neurol** 29:529-41.

McNaughton, B. L. (1980). Evidence for two electrophysiologically distinct perforant pathways to the fascia dentata. **Brain Res** 199:1-19.

McNaughton, B. L., and Barnes, C. A. (1977). Physiological identification and analysis of dentate granule cell responses to stimulation of the medial and lateral perforant pathways in the rat. **J Comp Neurol** 175:439-454.

Meldrum, B. S. (1975). Epilepsy and gamma-aminogutyric acid-mediated inhibition. **Int Rev Neurobiol** 17:1-36.

Michelson, H. B., Kapur, J., and Lothman, E. W. (1989). Reduction of paired pulse inhibition in the CA1 region of the hippocampus by pilocarpine in naive and in amygdala-kindled rats. **Exp Neurol** 104:264-71.

Mott, D. D., Xie, C. W., Wilson, W. A., et al. (1993). GABAB autoreceptors mediate activity-dependent disinhibition and enhance signal transmission in the dentate gyrus. **J Neurophysiol** 69:674-91.

Mouritzen Dam, A. (1980). Epilepsy and neuron loss in the hippocampus. **Epilepsia** 21:617-629.

Mouritzen Dam, A. (1982). Hippocampal neuron loss in epilepsy and after experimental seziures. **Acta Neurolog Scand** 66:601-42.

Munoz, M. D., Nunez, A., and Garcia-Austt, E. (1991). Frequency potentiation in granule cells in vivo at theta frequency perforant path stimulation. **Exp Neurol** 113:74-8.

Nadler, J., Perry, B., and Cotman, C. (1980). Selective reinervation of hippocampal area CA1 and the fascia dentata after destruction of CA3-CA4 afferents with kainic acid. **Brain Res** 182:1-9.

Nakajima, S., Franck, J. E., Bilkey, D., and Schwartzkroin, P. A. (1991). Local synaptic interactions between CA1 pyramidal cells and interneurons in the kainate-lesioned hyperexcitable hippocampus. **Hippocampus** 1:67-78.

Nobrega, J. N., Kish, S. J., and McIntyre Burnham, W. (1989). Autoradiographic analysis of benzodiazepine binding in entorhinal kindled rat brains. **Brain Res** 498:315-22.

Nobrega, J. N., Kish, S. J., and McIntyre Burnham, W. (1990). Regional brain [3H]muscimol binding in the kindled rat brain: a quantitative autoradiographic examination. **Epilepsy Res** 6:102-9.

Ogata, N. (1990). Pharmacology and physiology of GABA-B receptors. **Gen Pharmacol** 21:395-402.

Oliver, M. W., and Miller, J. J. (1985). Alterations of inhibitory processes in the dentate gyrus following kindling-induced epilepsy. **Exp Brain Res** 57:443-7.

Olney, J. W., Collins, R. C., and Sloviter, R. S. (1986). Excitotoxic mechanisms of epileptic brain damage. **Adv Neurol** 44:857-77.

Otis, T. S., and Mody, I. (1992). Differential activation of GABA-A and GABA-B receptors by spontaneuosly released transmitter. **J Neurophysiol** 67:227-35.

Peer, M. J., and McLennan, H. (1986). Pre- and postsynaptic actions of baclofen: blockage of the late synaptically evoked hyperpolarization of CA1 hippocampal neurons. **Exp Brain Res** 61:567-74.

Ramon y Cajal, S. (1893). Estructura del asta de Ammon. **Anat Soc Esp Histol Nat Madrid** 22:53-114.

Rassmussen, T. B. (1983). Surgical treatment of complex partial seizures: results, lessons, and problems. **Epilepsia** 24 (Suppl. 1):S65-S76.

Ribak, C. E., Bradburne, M., and Harris, B. (1982). A preferential loss of gabaergic, symmetric synapses in epileptic foci: a quantitative ultrastructural analysis of monkey cortex. **J Neurosci** 2:1725-35.

Ribak, C. E., Seress, L., and Amaral, D. G. (1985). The development, ultrastructure and synaptic connections of the mossy cells of the dentate gyrus. **J Neurocytol** 14:835-57.

Rich, K. M., Goldring, S., and Gado, M. (1985). Computed tomography in chronic seizure disorder caused by glioma. **Archives of Neurology** 42:26-27.

Robinson, G. B. (1991). Kindling-induced potentiation of excitatory and inhibitory inputs to hippocampal dentate granule cells. II. Effects of the NMDA antagonist MK-801. **Brain Res** 562:26-33.

Rogers, B. C., Barnes, M. I., Mitchell, C. L., and Tilson, H. A. (1989). Functional deficits after sustained stimulation of the perforant path. **Brain Res** 493:41-50.

Rutecki, P. A., Grossman, R. G., Armstrong, D., and Irish-Loewen, S. (1989). Electrophysiological connections between the hippocampus and entorhinal cortex in patients with complex partial seizures. **Journal of Neurosurgery** 70:667-675.

Sano, K., and Malamud, N. (1953). Clinical significance of sclerosis of the cornu ammonis. **Arch Neurol Psychiatry** 70:40-53.

Sass, K. J., Sass, A., Westerveld, M., et al. (1992). Specificity in the correlation of verbal memory and hippocampal neuron loss: dissociation of memory, language, and verbal intellectual ability. **J Clin Exp Neuropsychol** 14:662-72.

Sass, K. J., Spencer, D. D., Kim, J. H., et al. (1990). Verbal memory impairment correlates with hippocampal pyramidal cell density. **Neurology** 40:1694-7.

Scharfman, H. E., Kunkel, D. D., and Schwartzkroin, P. A. (1990). Synaptic connections of dentate granule cells and hilar neurons: results of paired intracellular recordings and intracellular horseradish peroxidase injections. **Neuroscience** 37:693-707.

Scharfman, H. E., and Schwartzkroin, P. A. (1990). Responses of cells of the rat fascia dentata to prolonged stimulation of the perforant path: sensitivity of hilar cells and changes in granule cell excitability. **Neuroscience** 35:491-504.

Schwartzkroin, P. A. (1994). Cellular electrophysiology of human epilepsy. **Epilepsy Res** 17:185-92.

Schwartzkroin, P. A., Turner, D. A., Knowles, W. D., and Wyler, A. R. (1983). Studies of human and monkey 'epileptic' neocortex in the in vitro slice preparation. **Ann Neurol** 13:249-57.

Segal, M. (1977). Afferents to the entorhinal cortex of the rat studied by the method of retrograde transport of horseradish peroxidase. **Exp Neurol** 57:750-65.

Sloviter, R. S. (1987). Decreased hippocampal inhibition and a selective loss of interneurons in experimental epilepsy. **Science** 235:73-6.

Sloviter, R. S. (1991a). Feedforward and feedback inhibition of hippocampal principal cell activity evoked by perforant path stimulation: GABA-mediated mechanisms that regulate excitability in vivo. **Hippocamus** 1:31-40.

Sloviter, R. S. (1991b). Permanently altered hippocampal structure, excitability, and inhibition after experimental status epilepticus in the rat: the "dormant basket cell" hypothesis and its possible relevance to temporal lobe epilepsy. **Hippocamus** 1:41-66.

Sloviter, R. S. (1992). Possible functional consequences of synaptic reorganization in the dentate gyrus of kainate-treated rats. **Neurosci Lett** 137:91-6.

Sloviter, R. S., and Damiano, B. P. (1981). On the relationship between kainic acid-induced epileptiform activity and hippocampal neuronal damage. **Neuropharmacology** 20:1003-11.

Sloviter, R. S., Sollas, A. L., Barbaro, N. M., and Laxer, K. D. (1991). Calcium-binding protein (calbindin-D28K) and parvalbumin immunocytochemistry in the normal and epileptic human hippocampus. **J Comp Neurol** 308:381-96.

Sommer, W. (1880). Erkrankung des Ammonshorns als aetiologisches Moment der Epilepsie. **Arch Psychiatr Nervenkr** 10:631-75.

Soriano, E., and Frotscher, M. (1989). A GABAergic axo-axonic cell in the fascia dentata controls the main excitatory hippocampal pathway. **Brain Res** 503:170-4.

Soriano, E., and Frotscher, M. (1994). Mossy cells of the rat dentat fascia are glutamate-immunoreactive. **Hippocampus** 4:65-9.

Spencer, D. D. (1994). Classifying the epilepsies by substrate. **Clin Neruosci** 2:104-9.

Spencer, D. D., Spencer, S. S., Mattson, R. H., and Williamson, P. D. (1984a). Intracerebral masses in patients with intractable partial epilepsy. **Neurology** 34:432-6.

Spencer, D. D., Spencer, S. S., Mattson, R. H., et al. (1984b). Access to the posterior medial temporal lobe structures in the surgical treatment of temporal lobe epilepsy. **Neurosurgery** 15:667-71.

Spencer, S. S., Spencer, D. D., Williamson, P. D., and Mattson, R. (1990). Combined depth and subdural electrode investigation in uncontrolled epilepsy. **Neurology** 40:74-9.

Spencer, S. S., Spencer, D. D., Williamson, P. D., and Mattson, R. H. (1982). The localizing value of depth electroencephalography in 32 patients with refractory epilepsy. **Ann Neurol** 12:248-53.

Steward, O. (1976). Topographic organization of the projections from the entorhinal area of the hippocampal formation of the rat. **J Comp Neurol** 167:285-314.

Storm-Mathison, J., Leknes, A. K., Bore, A. T., et al. (1983). First visualization of glutamate and GABA in neurones by immunocytochemistry. **Nature** 301:517-20.

Stringer, J. L., and Colbert, C. M. (1994). Analysis of field potentials evoked in Ca1 by angular bundle stimulation in the rat. **Brain Res** 641:289-94.

Stringer, J. L., and Lothman, E. W. (1989). Repetitive seizures cause an increase in paired-pulse inhibition in the dentate gyrus. **Neurosci Letters** 105:91-95.

Strum, R. D., and Kirk, D. E. (1989). **First Principles of Discrete Systems and Digital Signal Processing**. New York: Addison-Wesley Publishing Co., Inc.

Sutula, T. P. (1990). Experimental models of temporal lobe epilepsy: new insights from the study of kindling and synaptic reorganization. **Epilepsia** 31(Suppl. 3):S45-S54.

Sutula, T. P., Cascino, G., Cavazos, J., and Scott, G. (1988). Mossy fiber synaptic reorganization in the epileptic human temporal lobe. **Ann Neurol** 26:321-330.

Swanson, L. W., and Cowan, W. M. (1977). An autoradiographic study of the organization of efferent connections of the hippocampal formation in the rat. **J Comp Neurol** 172:49-84.

Tauck, D., and Nadler, J. V. (1985). Evidence of functional mossy fiber sprouting in the hippocampal formation of kainic-acid treated rats. **J Neurosci** 5:1016-22.

Thalman, R. H., and Ayala, G. F. (1982). A late increase in potassium conductance follows synaptic stimulation of granule neurons in the dentate gyrus. **Neurosci Lett** 29:243-248.

Thompson, S. M., Capogna, M., and Scanziani, M. (1993). Presynaptic inhibition in the hippocampus **Trends Neurosci** 16:222-7.

Thompson, S. M., and Gahwiler, B. H. (1989). Activity-dependent disinhibition I. Repetetive stimulation reduces IPSP driving force and conduction in the hippocampus in vitro. **J Neurophysiol** 61:501-11.

Thompson, S. M., and Gahwiler, B. H. (1992). Activity dependent disinhibtion. III. Desensitization and GABA-B receptor-mediated presyaptic receptors in the hippocampus in vitro. **J Neurophsyiol** 61:524-33.

Tuff, L. P., Racine, R. J., and Adamec, R. (1983). The effects of kindling on GABA-mediated inhibition in the dentate gyrus of the rat. I. Paired pulse depression. **Brain Research** 277:79-90.

Urban, L., Aitken, P. G., Crain, B. J., et al. (1993). Correlation between function and structure in "epileptic" human hippocampal tissue maintained in vitro. **Epilepsia** 34:54-60.

Urban, L., Aitken, P. G., Friedman, A., and Somjen, G. G. (1990). An NMDA-mediated component of excitatory synaptic input to dentate granule cells in 'epileptic' human hippocampus studied in vitro. **Brain Res** 515:319-22.

Uruno, K., O'Connor, M. J., and Masukawa, L. M. (1994). Alterations of inhibitory synaptic responses in the dentate gyrus of temporal lobe epileptic patients. **Hippocampus** 4:583-593.

Van Hoesen, G. W., Pandya, D. N., and Butters, N. (1975). Some connections of the entorhinal area (area 28) and peripheral (area 35) cortices of the rhesus monkey II. Frontal lobe afferents. **Brain Res** 95:25-35.

VanLandingham, K. E., and Lothman, E. W. (1991a). Self-sustaining limbic status epilepticus. I. Acute and chronic cerebral metabolic studies: limbic hypermetabolism and neocortical hypometabolism. **Neurology** 41:1942-9.

VanLandingham, K. E., and Lothman, E. W. (1991b). Self-sustaining limbic status epilepticus. II. Role of hippocampal commissures in metabolic responses. **Neurology** 41:1950-7.

Voskuyl, R. A., and Albus, H. (1987). Enhancement of recurrent inhibition by angular bundle kindling is retained in hippocampal slices. **Int J Neurosci** 36:153-66.

White, W. F., Nadler, J. V., and Cotman, C. W. (1979). Analysis of short-term plasticity at the perforant path-granule cell-synapse. **Brain Res** 178:41-53.

Williamson, A., McCormick, D. A., Shepherd, G. M., and Spencer, D. D. (1990). Intracellular recordings from epileptic human dentate granule cells show evidence of hyperexcitability [Abstract]. **Epilepsia** 31:625.

Williamson, A., and Spencer, D. D. (1994). Electrophysiological characterization of CA2 pyramidal cells from epileptic humans. **Hippocampus** 4:226-37.

Williamson, A., Spencer, D. D., and Shepherd, G. M. (1993b). Comparison between the membrane and synaptic properties of human and rodent dentate granule cells. **Brain Res** 622:194-202.

Witter, M. P., Van Hoesen, G. W., and Amaral, D. G. (1989). Topographical organization of the entorhinal projection to the dentate gyrus. **J Neurosci** 9:216-28.

Wood, J. D. (1975). The role of gamma-aminobutyric acid in the mechanism of seizures. **Progr Neurobiol** 5:77-95.

Yamada, N., and Bilkey, D. K. (1991). Kindling-induced persistant alterations in the membrane and synaptic porperties of CA1 pyramidal neurons. **Brain Res** 561:324-31.

Yeckel, M. F., and Berger, T. W. (1990). Feedforward excitation of the hippocampus by afferents from the entorhinal cortex: redefinition of the role of the trisynaptic pathway. **Proc Natl Acad Sci U S A** 87:5832-6.

Zhao, D., and Leung, L. S. (1992). Hippocampal kindling induced paired-pulse depression in the dentate gyrus and paired-pulse facilitation in CA3. **Brain Res** 582:163-7.

HARVEY CUSHING / JOHN HAY WHITNEY
MEDICAL LIBRARY

MANUSCRIPT THESES

Unpublished theses submitted for the Master's and Doctor's degrees and deposited in the Medical Library are to be used only with due regard to the rights of the authors. Bibliographical references may be noted, but passages must not be copied without permission of the authors, and without proper credit being given in subsequent written or published work.

This thesis by has been used by the following persons, whose signatures attest their acceptance of the above restrictions.

NAME AND ADDRESS DATE